Responses to comments from anonymous referee #1

Original comments are in **black.** Our point by point responses are in **blue**. All changes in the context have been highlighted with yellow background.

This paper summarises a wintertime observation-modelling study in a small lake on the Qinghai-Tibet plateau. The thermodynamics of the lake is analysed in an air/ice/water column by using in-situ measurements and thermodynamic model HIGHTSI, earlier applied for several studies on lake and sea ice all over the Northern Hemisphere. Energy balance at the top and bottom of the lake ice shows features typical for the conditions of the "third pole" but unusual elsewhere on the globe. The manuscript presents unique observations and modelling results in the unique environmental conditions of the Qinghai-Tibet plateau. I have enjoyed reading it, meeting a lake whose thermodynamics seem to differ crucially from all other lakes I have met in earlier studies. In my opinion, the manuscript has potential to become an outstanding paper that can point a way to future studies for understanding the impact of changing climate on the cryosphere and its feedbacks to atmosphere over this area of global importance. In the manuscript there is sufficient material, good methods and well posed research questions and the structure of the manuscript is good. However, this rich material deserves better presentation in order to be understood by researcher colleagues and general reader.

Several questions arise when reading the paper, concerning not only details but also more general aspects of the impact of lakes on the "third pole". There is both general background information and details about the studied lake but it might be possible to better tie these together at the regional (QTP) level. Unfortunately, it is not always possible to understand what the authors want to say, due to poorly formulated, too general or unfinished statements and problems of English language. The paper should be rewritten in a more focused way by removing material that is not essential to the study.

Next, I will present some general comments on how I understood, based on your manuscript, the unique properties that determine the lake thermodynamics and mass balance over the plateau and in the studied lake. More specific comments are written into the manuscript pdf using Adobe reader. I also hope the authors will have a possibility to request linquistic support in order to improve the English in the paper.

Thank you for the comments. We have responded your general and point by point comments below.

During the revision, we removed the dispensable materials and statements, reformulated the manuscript structure, and improved the English readability by a native speaker. All parts are now bound up with the key issues of the manuscript.

——

General comments or how I understood the unique properties that influence the lake thermodynamics and mass balance

A small lake with the surface area of 1.5 hectars, shallow with mean depth of 2.5m at high altitude of ca. 4000m. At the bottom: talik and permafrost.

Strong, gusty wind prevails during winter. Clear sky conditions, strong solar radiation with the daily maxima up to 1140 Wm-2. Strong LW cooling to space at the surface. In the air, small humidity on average 34%. Yearly precipitation is 353 mm but potential evaporation is 1613 mm. No rivers flow to/from the lake. Subsurface inflow/outflow?

Sublimation of lake ice - up to 40 % of lake ice disappears to air during winter. Small ice surface melting in spring. Melting at the ice bottom due to penetrating solar radiation.

Possibly falling snow is blown away from ice surface. Dust gathers on ice in the end of winter. These lead to 1) smaller albedo 2) no thermal insulation by snow.

Penetration of SW radiation into the (transparent?) ice and water below, absorption in ice and water. Melting of ice from bottom in interior ice layers. Convection under ice. Diurnal cycles of freezing and melting, ice temperatures.

——

Did I understand correctly the main features? Would you consider developing this kind of summary a bit further, perhaps presenting a comparison (Table, Figure?) with an Arctic lake you have been studying earlier? This would illustrate the unique nature of lakes in your study area and perhaps highlight open questions that call for further research. Such a comparison might suit the concluding section. Also it would be interesting see comments on what is required from a model to correctly simulate lake thermodynamics in these conditions. HIGHTSI works but would for example the bulk lake model FLake be able to simulate the QTP lakes?

Yes, the main features you summarized above are correct. We have incorporated such kind of a summary in the manuscript.

We have added in the conclusion section comparisons between the shallow QTP lake and a lake in the high Arctic (Orajärvi) to emphasize the uniqueness of QTP shallow lakes and their climate characteristics (Table R1).

From a modeling perspective, the radiation reflection, absorption, and transmission should be constrained accurately since (1) extremely low surface albedo was reported by Li et al. (2018, J Glaciol) in large deep QTP lakes, and it needs confirmation in small shallow lakes; (2) the impact of deposited fine sand/dust on ice surface albedo should be evaluated properly; (3) the penetration of solar radiation is believed to strongly affect the water-to-ice heat flux (F_w) that controls the basal growth and melt of ice. Schemes and parameterizations of solar radiation in ice (albedo, extinction, and transmission) need further validation using in situ investigations. Furthermore, F_w needs more careful treatment, and is a time dependent variable in these lakes. Using a constant F_w (e.g. in FLake) does not give reasonable results compared with observations.

We did not conduct experiments using FLake model, but we think the above-mentioned concerns should also be taken in mind since HIGHTSI and FLake use similar key formulations for simulation of ice thickness. Particularly, new schemes for F_w should be proposed regarding the under-ice radiation and hydro-thermodynamic processes. These call for many more field observations and modeling efforts.

Table R1 Comparisons of lake and meteorological features between Lake BLH-A and an Arctic lake (Lake Orajärvi)

Items	Lake BLH-A	Lake Orajärvi**
Surface area	0.015 km2	11 km2
Mean depth	2.5 m	4.4 m
Altitude	4600 m	182 m
Annual precipitation	353 mm	500 mm
Annual evaporation	1613 mm	450 mm (Venäläinen et al., 2005)
Air temperature*	-10.6 ℃	-9~-10 ℃
Wind speed*	6.5 m/s	2.3 m/s
Relative humidity*	34%	85%~87%
Short-wave radiation*	390 W/m^2	41-46 W/m^2
Long-wave radiation*	180 W/m^2	240-260 W/m^2
Net long-wave radiation*	-89 W/m^2	-19~-27 W/m^2
Snow cover	Negligible (light dust)	Up to over 30 cm
Ice surface sublimation	30 cm	Negligible
Ice structure	Congelation ice	Snow-ice + superimposed ice + congelation ice

*averaged over the entire ice season

**data during winters of 2010-2012 were used for statistics

According to the Global Surface Water Explorer, global-surface-water.appspot.com, during the last decades there is a tendency to new permanent and seasonal small lakes and ponds to appear, not disappear, over the plateau. In their maps, Lake BLH-A has got permanent, new permanent and new seasonal pixels. How do you explain the dynamics of your lake (over the whole year, not only in winter conditions that you discuss here), that evidently loses yearly a significant amount of water by evaporation/sublimation but still stays well alive? Large-scale permafrost melting, something else? Would be interesting to discuss the related aspects from the point of view of the possible impact of the (new) small lakes in the weather and climate of QTB and connections to even larger areas. Anyway, the area and mass of water in the lakes and ponds is currently relatively small?

Actually, we do not know very well the hydrology or water balance of Lake BLH-A but we believe it is permanent and its age is around 900 years according to environmental isotopic dating of its sediment core (Niu et al., 2011, Geomorphology). It holds water all year around and its surface area shows an increasing trend and many new lakes have appeared in the Beiluhe Basin during recent decades on the basis of Google Earth images and SPOT data (e.g. Luo et al., 2015, Sci Bull.).

Additionally, a very minor gully flows into Lake BLH-A during summertime without outflow, and there is no surface inflow/outflow during the freezing period. Although P-E-WSD (annual precipitation–evaporation–wintertime subsurface discharge) is negative, this can be compensated by the supra-permafrost inflows and slope runoff (confluence) during thaw seasons (especially summer) resulting from precipitation, glacier melting, and underground ice melting (Pan et al., 2017, J Hydrol; also Lei et al., 2017, GRL; Zhang et al., 2014, Sci Bull.). According to field investigations by Pan et al (2017) in similar thermokarst lakes, a large portion of lake water storage change is because of the supra-permafrost discharge resulting from precipitation, and the recent lake expansion is linked with increasing supra-permafrost discharge especially with an increasing trend in precipitation in QTP.

More results are coming since our group is currently planning and conducting field campaigns on lake water balance dynamics in Beiluhe Basin.

In section 4.3, we have added a general statement on the physics governing the lake water balance through a hydrological year. But the thorough discussion above is not necessary since we focus on lake ice thermodynamics.

Actually, the area and mass of water in these very small shallow lakes and ponds are currently relatively small, but the number of small lakes and their total shoreline length, which are of importance for lake environment, ecology and benthic community, account for >90% of those of total lakes over QTP. Due to climate warming, permafrost and glacier melting and rising precipitation result in generation of many more new small shallow (thermokarst) lakes, especially in continuous permafrost regions. Individual lakes and lake networks in turn accelerate the surrounding permafrost degradation through lateral heat erosion, and also alter the hydrological processes and patterns in permafrost regions.

Lake ice phenology/thickness is demonstrated to be the principal driver of ecological change in Arctic lakes and ponds (Griffiths et al., 2017, PLOS One), and is also expected to have an impact on the duration of the lake bank lateral collapse. Remote sensing products have shown significant spatial variability of lake ice phenology evolution (of climatological importance) over QTP (Kropáček et al., 2013, TC). Using the HIGHTSI model, lake ice evolution and lake water loss by sublimation can be estimated over QTP. Moreover, our study discusses the wintertime lake-atmosphere heat and moisture exchanges that are not well known up to now due to scarce field observations. In the future, schemes for freeze-up and break-up dates can be incorporated to HIGHTSI. After a solid validation, a deep insight into atmosphere-ice-water heat and mass balance over QTP can be achieved.

Specific comments — written into the manuscript pdf.

L20: Rephrased to "The growth and decay at the ice bottom dominated the seasonal evolution of the lake ice."

L21: deleted.

L22-23: Rephrased to "Simulation results matched the observations well with respect to ice mass balance components, ice thickness, and ice temperature."

L24: "freezing air temperature" → "negative air temperature".

L31-33: deleted. But L21-22 have been rephrased to "Basal growth and melt dominated the seasonal evolution of lake ice, but also surface sublimation was crucial for ice loss, accounting for up to 40% of the maximum ice thickness. Sublimation was also responsible for 41% of the lake water loss during the ice-covered period."

L36: "freezing climate"→ "cold climate".

L37: rephrased to "It owns thousands of lakes covering a total area of approximately 40,700 km^2 (1.4% of the QTP area) and accounting for about 50% of lakes located in China (Zhang et al., 2014)."

L47: We meant that the number and total area of QTP lakes show annual variation. To be clearer, we have rephrased it to "The number and surface area of the lakes varies inter-annually"

L51-52: deleted (including the cited reference Yang et al. 2015).

L59-60: deleted.

L62-65:

Q: Rephrase (something about the need of modelling to understand observations?) or skip. Remote sensing observations are clearly out of context

A: Rephrased to "Because of sparse field observations, there is an increasing need of models and parameterizations to better understand the lake-air interaction and lake thermal regime (Kirillin et al., 2017; Wang et al., 2015; Wen et al., 2016)."

L72: delete "Nevertheless".

L75: delete "of years".

L76-77:

Q: please specify "High-resolution remote sensing techniques and products were deployed tentatively to …"

A: Further, moderate- to high-resolution remote sensing techniques and products, such as MODIS and ENVISAT-ASAR, have been found to be promising and convenient tools for large-scale QTP lake ice research (Kropáček et al., 2013; Tian et al., 2015).

L81: We have added the reference "Yang et al. 2013".

L82-85:

Q: Good! Please check that your conclusions tell about reaching these objectives.

A: Done, we have revised the conclusions to state reaching these goals.

L102: Q: At which altitude is this lake located?

A: The lake is 4,600 m above the sea level. We indicated it in the updated version.

L106: Yes, it is a unit of concentration. The TDS (total dissolved solids) is 1.30 g L^{-1}, corresponding to 1.30 kg m^{-3}.

L109: Q: please specify on "its disturbance to surrounding frozen ground"

A: heat intrusion from the lake water to surrounding permafrost.

L115-123:

Q: Are all your measurements listed here: T_ice, T_water, T_sediment, T_air, D_f D_b H_b, H_s. Are there temperature profiles or 4 values?

A: Yes, there are temperature profiles for T_ice, T_water, T_sediment, and T_air, etc. We have added these nomenclatures to the corresponding observed variables.

L121-123:

Q: Perhaps this is explained in Huang et al. 2016 but might be good to tell here a bit more details about the temperature and position measurements. How do you obtain the vertical positions - measure everything starting from the bottom perhaps?

A: We added new text reading: “a floater was designed and deployed onto the water surface. A thermistor cable was fixed to the floater to measure the ice-water temperature at 5 cm intervals. An upward looking ultrasonic sensor was also fixed to the floater and positioned at 100 cm depth to monitor the depth of the ice-water interface. A downward looking ultrasonic sensor was fixed to a steel pipe, which had been inserted into the lake sediment by ~60 m, to monitor the position/depth of ice surface.”

For a better clarity and illustration, we added also a sub-figure describing the instrumentation in Figure 1.

L136: Q: What means dry here? Without snow/melt water/...?

A: Yes, it is, without snow and melt-water, we modified the text accordingly.

L139: Added.

L183-184: Q: Is this an average between sunrise and sunset, or 24h?

A: It is an average over the whole day (24 h).

L185: Q: Local time? What about 7-8, 19-20?

A: Corrected by “during daytime (8:00-19:00), and nighttime (19:00-8:00)”.

L202: Changed to “Huang et al., 2019”. And this reference was added to the reference list.

L205: were→ are.

L213: Q: Your components are 4: surface ice melting and sublimation, bottom freezing and melting?

A: Yes, we updated the sentence. The bottom freezing and melting contribute to the bottom evolution.

L221: Yes, it is the modeled ice bottom depth.

L228: Yes, it is local time.

Table 2:

Q: Table 2 shows model-observation validation for ice surface and bottom heights and their difference in cm? Does the total mass balance mean ice thickness here? Otherwise it is not easy to understand a balance in cm. Please use consistent names.

A: Yes, it is quantified in unit [cm]. The total mass balance means the ice thickness. In order to be easy to understand, we used surface height, bottom height, and the ice thickness in the revised version.

L240: rephrased to “when it revealed some cycles of daytime-melting and nighttime-freezing at the surface.”

L263: rephrased to “. Therefore, it was divided into three parts: …”

L267: added.

L274: corrected.

L275: Q: Ice surface to atmosphere? Atmospheric surface layer?

A: No, it is a thin ice layer below ice skin surface.

L278: added.

L281: For the surface heat balancing → According to the surface heat balance

L282: corrected.

L287: internal melting in way of gas pore expansion → interior melt in a manner of gas pore expansion

L297: added.

L299: have been carrying out → have been performed

L300: deleted.

L303: added.

L313: differ from → different from

L314: was → is

L323: of → to be

L329-331: deleted.

L348: rephrased to "Diurnal changes in turbulent heat fluxes, however, are large and commonly seen in high latitude and high altitude lakes".

L351: are → were

L352-354: rephrased to "At seasonal scale, the Q_h and Q_{le} over lake ice are approximately 40%-60% lower than values during ice-free seasons, demonstrating the role of ice as an insulator.".

L377-383:

Q: You might compare this to what happens during the ice-free period that might indicate why the lake is still there. You probably have such measurements available, published earlier?

A: Actually, the lake level decreases continuously (totally by ~ 0.5 m) from Aug/Sept to May/Jun of the next year (including the ice-covered seasons) due to subsurface seepage, evaporation, and ice sublimation, and increases rapidly (totally by ~ 0.5 m) due to heavy precipitation and melting glaciers (induced surface and supra-permafrost recharge) during warm seasons (Jul. to Aug.) (Lin et al., 2017; Pan et al., 2017). Consequently, over the entire hydrological year, the lake water loss through surface/sub-surface flows and evaporation/sublimation (during ice-covered period) can be roughly compensated/offset by the precipitation and subsurface/surface inflow during warm seasons. Therefore, these shallow lakes can be still there.

Since the water balance during ice-free seasons is somehow out of context, we have added only brief info to the updated manuscript as well as some new citations.

L380: Q: please remind the reader what is talik

A: It is a layer of year-round unfrozen ground. We added in the revised manuscript.

L384: 5. Summary and conclusion

Q: This is a good summary of your findings. However, discussion of more general aspects of the impact of lakes on QTP in the conditions of changing climate could be added, also an outlook to further studies might be given. Please consider the idea given in my general comments to summarise and compare the unique features of your lake v.s. another, e.g. Arctic lake using a figure or table.

A: We have added comparison with other lake, and general characteristic of this QTP lake based on your summary and suggestions. The new text reads: "Comparisons with an Arctic lake revealed the uniqueness of QTP lakes especially with respect to the atmospheric forcing, lake geometry, ice cover (free of snow), and under-ice hydro-thermodynamics (Table 4). These features challenge the existing lake ice models that are mainly developed for Arctic and temperate regions. However, present modeling experiments indicated that HIGHTSI could yield reasonable results in terms of the surface and bottom freezing/ablation and ice thermodynamics."

And we also indicated our future work regarding estimation of wintertime lake sublimation over-QTP, investigating physics governing under-ice heat flux, and light transfer within air-ice-water column, etc. These future investigations are vital to understand QTP lake thermodynamics and accurately constrain lake (ice) models, like FLake, HIGHTSI, etc.

L424: Q: Wouldn't it be possible to measure reflected SW radiation on ice? Perhaps also the other radiative fluxes? If Li et al, 2018 already reports such measurements, perhaps an abledo value could be mentioned here?

A: In fact, we carried out TriOS spectro-radiometers measurement during 2012-2013 season in the lake but unfortunately without a major success due to instrumental malfunction. Only 10-hours daytime incident and reflected SW radiative fluxes were obtained and a surface albedo of about 0.6-0.65 was derived (ice thickness= 45 cm, air temperature= -3.4 ℃). This observed value agreed well with parameterized albedo in HIGHTSI when modelled ice was around 45 cm. The albedo measurements by Li et al (2018) are from other large and deep lakes in QTP. The unprecedentedly small surface albedo was around 0.2 when ice was 60 cm. For our lake due to the impact of ice texture (gas bubbles), color, deposited sand, the surface albedo is higher than 0.2, but when ice was thinner than 10 cm, the parameterized surface albedo was around 0.2. We have modified the text and added the albedo values, accordingly.

L437: meteorology → meteorological forcing

Table 2: Corrected.

Figure 1:

Q: Please consider to show, as in the presentation at Lake17 workshop, a satellite map where the lake is seen. More interestingly, please explain what is seen in the photo on the lake ice - looks like deposition ice but perhaps it is something else?

A: The map is updated accordingly.

Figure 2: Q: Here and in the following figures: would it be possible to replace the julian days with year/month/day format?

A: Done.

Figure 5: Corrected.

Figure 7: Corrected.

Figure 8: Corrected.

Figure 11: Corrected.

Figure 12: Corrected.

You may have forgotten one reference to your own studies, possibly relevant for this manuscript:

Yang, Y., Cheng, B., Kourzeneva, E., Semmler, T., Rontu, L., Leppäranta, M., Shirasawa, K. & Li, Z. J. 2013: Modelling experiments on air–snow–ice interactions over Kilpisjärvi, a lake in northern Finland. Boreal Env. Res. 18: 341–358.

Added.

Other changes

(1) We improved the English readability by a native speaker, many definite/indefinite articles, singular/plural nouns, simple phrases, and sentence patterns have been modified, but are not shown in this response letter.

(2) Julian dates have been removed and replaced by calendar in the text and in all figures.

(3) All “2010/2011” have been reformed to “2010–2011”.

(4) Lines 98-101 (and references therein) were removed since it is not essential to the topics.

(5) Line 105: delete “with a stable water level through the year”, and “fresh” → brackish”.

(6) Line 106-107: delete “Submerged plants grow abundantly in the lake sediment throughout the year.”, since it is not essential to the topics.

References listed in the above response:

Griffiths, K., Michelutti, N., Sugar, M., Douglas, M. S. V., Smol, J. P., 2017. Ice-cover is the principal driver of ecological change in High Arctic lakes and ponds. PLoS ONE, 12(3): e0172989, doi:10.1371/journal.pone.0172989.

Kirillin, G., Wen, L., and Shatwell, T.: Seasonal thermal regime and climatic trends in lakes of the Tibetan Highlands, Hydrol. Earth Syst. Sci., 21, 1895-1909, 2017.

Kropáček, J., Maussion, F., Chen, F., Hoerz, S., and Hochschild, V.: Analysis of ice phenology of lakes on the Tibetan Plateau from MODIS data, The Cryosphere, 7, 287-301, 2013.

Lei, Y., Yao, T., Yang, K., Sheng, Y., Kleinherenbrink, M., Yi, S., Bird, B. W., Zhang, X., Zhu, L., and Zhang. G.: Lake seasonality across the Tibet Plateau and their varying relationship with regional mass balance and local hydrology, Geophys. Res. Lett., 44, 892-900, doi: 10.1002/2016GL072062.

Li, Z., Ao, Y., Lyu, S., Lang, J., Wen, L., Stepanenko, V., Meng, X., and Zhao, L.: Investigations of the ice surface albedo in the Tibetan Plateau lakes based on the field observation and MODIS products, J. Glaciol., doi: 10.1017/jog.2018.35, 2018.

Luo, J., Niu, F., Lin, Z., Liu, M., and Yin, M.: Thermokarst lake changes between 1969 and 2010 in the Beilu River Basin, Qinghai-Tibet Plateau, Chinese Sci. Bull., 60(5), 556-564, 2015.

Pan, X., Yu, Q., You, Y., Chun, K. P., Shi, X., and Li, Y.: Contribution of supra-permafrost discharge to thermokarst lake water balances on the northeastern Qinghai-Tibet Plateau, J. Hydrol., 555, 621-630, 2017.

Tian, B., Li, Z., Engram, M. J., Niu, F., Tang, P., Zou, P., and Xu, J.: Characterizing C-band backscattering from thermokarst lake ice on the Qinghai-Tibet Plateau, ISPRS J. Photogramm. Remote Sens., 104, 63-76, 2015.

Venäläinen A, Tuomenvirta H, Pirinen P, Drebs A. 2005. A Basic Finnish Climate Data Set 1961-2000 – Description and Illustrations. Finnish Meteorological Institute Reports 5.

Wang, B., Ma, Y., Chen, X., Ma, W., Su, Z., and Menenti, M.: Observation and simulation of lake-air heat and water transfer processes in a high-altitude shallow lake on the Tibetan Plateau, J. Geophys. Res., 120, 12327-12344, 2015.

Wen, L., Lyu, S., Kirillin, G., Li, Z., and Zhao, L.: Air-lake boundary layer and performance of a simple lake parameterization scheme over the Tibetan highlands, Tellus A, 68, 31091, doi:10.3402/tellusa.v68.31091, 2016.

Zhang. G., Yao, T., Xie, H., Zhang, K., and Zhu, F.: Lakes' state and abundance across the Tibetan Plateau, Chinese Sci. Bull., 59(24), 3010-3021, 2014.

Responses to comments from anonymous referee #2

Original comments are in **black.** Our point by point responses are in **blue**. All changes in the context have been highlighted with yellow background.

The paper focused on seasonal lake ice mass and energy balance over a small lake in Tibetan Plateau with thousands of lakes. Owing to the harsh environment, the Qinghai Tibetan lakes are very sparsely covered by in situ measurements and little studied. With a case study observations and numerical simulation, the manuscript showed the interesting and useful information about the lake ice thermodynamics and heat and mass balance during ice-covered season in the Qinghai Tibetan Plateau, but the work and the manuscript should be checked carefully. Therefore, in my opinion, it should be published after moderate revisions. Specific comments as follows:

L15-16 What's the relationship between ice-covered lakes in the plateau and monsoon systems in winter?

Actually, here we meant that the lake-rich QTP, rather than lakes in QTP, has impacts on monsoon systems.

Previous studies have indicated that QTP contains the freshwater resources for 2/3 of the population in Asia, and QTP can affect the Asian monsoon system through the exchange of heat and moisture between the Earth surface (including lakes) and atmosphere, driven by the large scale atmospheric circulations (e.g. Li et al., 2016, *J. Hydrol.*).

In general, water and moisture transport and their interactions with QTP land topography under the influence of strong ABL circulation are the driving force of QTP on Asian monsoon system. In winter, QTP is cold so the water and moisture transportation is much reduced, instead evaporation and sublimation from ice-covered lakes has been observed (Huang et al., 2016; Li et al., 2016 *JGR*), but the linkage between ice-covered lakes in the plateau and monsoon systems in winter remains unclear and still need to be investigated.

L24-25 The author draws the conclusion that strong solar radiation, consistent freezing air temperature, and low air moisture were the major driving forces controlling the seasonal ice mass balance. The wind is quite strong including frequent gusts. It is quite important to the calculation of latent heat flux. How about wind effects on the seasonal ice mass balance?

Prevailing strong wind is vital factor influencing the ice mass balance because it increases the turbulent heat exchange between ice surface and near-surface atmosphere and contributes to ice surface ablation. The effect of wind on seasonal ice mass balance has been investigated before (e.g. Huang et al., 2016, *Ann. Glaciol.*) through sensitivity tests. We have concluded that both sensible and latent heat fluxes are crucial components for heat budgets for ice cover. We have added following text in the revised manuscript: "Strong solar radiation, consistent negative air temperature, low air moisture, and prevailing strong winds were the major driving forces controlling the seasonal ice mass balance."

L32 Ice surface sublimation could account 41% of lake water loss in ice season. Can we know its contribution in the annual water balance?

Yes, we can make the calculation. The inter-annual water balances of small lakes have been investigated before. According to multiyear investigations on lake water level in nearby two similar small lakes (Pan et al., 2017, *J. Hydrol.*), the water level of those small lakes decreases continuously from September to the June of the following year with a magnitude of about 0.5 m. The water loss includes subsurface seepage, evaporation, and sublimation of ice. During rest of the year: July-August, the lake water level increases rapidly due to surface and supra-permafrost recharge induced by heavy precipitation and runoff of melting glaciers with a total water level increase of about 0.5 m (Lin et al., 2017; Pan et al., 2017). So the annual water balances of those lakes remain stable. According to Pan et al.,(2017), the annual lake water loss (~ 620 mm) consists of evaporation during ice-free seasons (~340 mm, 55%), ice sublimation during ice-covered seasons (260 mm, 42%), and lateral seepage (20 mm, 3%) with negligible vertical seepage.

The contribution of ice surface sublimation on annual water balance is added in the revised manuscript section 4.3. The new text reads:

"The surface evaporation/sublimation hence accounts for 41% of lake water loss during the ice-covered period and for 42% of annual water loss (Pan et al., 2017)."

L94-95 "During years 2004-2014, the mean annual air and ground temperatures varied from -2.9 _C to -4.1 _C and from -1.8 _C to -0.5 _C, respectively". How could ground temperature increase 1.3 _C and mean annual air temperature decrease 1.2 _C during 11 years? And the warming rate is quite fast.

The original description was incorrect due to poor language formulation. The corrected description reads: "During years 2004-2014, the annual mean air temperature ranged between -4.1 ℃ and -2.9 ℃, and the annual mean ground temperature between -1.8 ℃ and -0.5 ℃".

L96-97 "precipitation ranged from 229 to 467 mm (average: 353 mm), while the annual mean potential evaporation ranged from 1588 to 1626 mm " VS L103 "The lake is perennially closed without rivers or streams flowing into and out of it." How did the lake survive with huge vaporation and less precipitation? How did the lake area and level respond to the rapid increase of precipitation?

Yes, a very minor gully flows (negligible recharge) into Lake BLH-A during summertime without outflow, and there is no surface inflow/outflow during freezing period. Although P-E-WSD (annual precipitation–evaporation–wintertime subsurface discharge) is negative, this can be compensated by the supra-permafrost inflows and slope runoff (confluence) during thaw seasons (especially summer) resulted from precipitation and glacier melting (Pan et al., 2017, J Hydrol; Lei et al., 2017, GRL). According to Pan et al (2017) field investigations in similar thermokarst lakes, a large portion of lake water storage change is because of the supra-permafrost discharge resulting from precipitation. The annual total loss can be roughly offset by the total recharge, therefore, the lake survives and stabilizes.

L110 What's the effects of plenty of gas bubbles on albedo as showed in Figure 1? Does it include in the simulation?

In general gas bubbles affect the ice interior texture, reflection and back-scattering of the light as well as roughness of ice-water interface. We would need to have incoming and reflected spectral solar radiative fluxes measurement to identify the impact of gas bubbles on surface albedo, which we were not able to carry out during 2010/2011 field campaign. We are not aware of an albedo parameterization that takes into account the effect of gas bubbles on ice surface. In other respects, the albedo scheme we applied is a sophisticated one, taking into account temperature, snow and ice thickness, solar zenith angle, and atmospheric properties, and distinguishing between visible and near-infrared albedos values (Briegleb et al., 2004).

L128 May I think the other two years' experiments failed? Why?

The other two years (ice seasons) mainly suffered, from time to time, the instrumental malfunction. Therefore, we focus on modelling experiments only for 2010/2011 season.

L142 The incident longwave radiation Ql is missed in equation (1), and the direction of the upward longwave radiation should be wrong. In this case, how about the simulated results?

The equation has been corrected accordingly.

The observed average down-welling Ql was 177 W m^{-2} during daytime (8:00-19:00, local time) and 180 W m^{-2} during nighttime (19:00-8:00), respectively. Table 3 gave the monthly mean net long-wave radiative flux (i.e. $Ql–\varepsilon\sigma T^4$) .

L162 The bulk transfer coefficient for water vapor is vital for Qle calculation. It varies with wind, stability and the type of landscape. How does it set in the calculation?

The effect of roughness lengths for momentum and heat/moisture transfer as well as the effects of ABL stratification were taken into account in the calculation of the turbulent surface fluxes of heat and moisture based on the Monin-Obukhov similarity theory (Launiainen, 1995; Launiainen and Cheng, 1995; Launiainen and Cheng,1998). Same approach has been applied to estimate sensible and latent heat fluxes between lake and atmosphere in large QTP lakes (Wang et al., 2015 *JGR*; Li et al., 2016 *Theor*

Appl Climatol).

L178 Undoubtedly, the air temperature between the two sites are highly correlated. What's difference between them? Could air temperature over lake surface show the lake characterises?

Yes, the air temperatures between the two sites are highly correlated. The average difference is about 0.3 ℃. We added this number in the revised manuscript.

The air temperature over a lake surface has a strong linkage associated with freeze up and breakup of the lake ice due to its strong cooling and warm effect.

We believe the air temperature observed in the floater located near the centre of the lake well represents the general temperature characteristics over the lake. We assume that the air temperature over a lake is not as sensitive as latent/sensible heat and moisture flux to surrounding land surface changes during wind direction changes.

L264-266 The percentage of solar radiation absorbed by lake surface is main factor to decide the Qss. Could you show more information about it? How to get the percentage of Qsi and Qsw? Are they fixed?

In HIGHTSI, very sophisticated schemes were used to quantify the light transfer in air-ice column. Within ice layer, two-layer model were usually used taking into account a thin surface ice layer (coefficient i_0) that is different from the ice layer below with respect to optical properties (Maykut & Perovich, 1987).

$$q_i(z,t) = i_0(1-\alpha_i)Q_s e^{-\kappa_i(z-\bar{z})},$$

where i_0 is defined as the fraction of the wavelength-integrated incident irradiance transmitted through the top layer of the ice, and parameterized as a function of sky conditions (cloud fraction, C) and ice colour (Grenfell & Maykut 1977; Perovich 1996). Accordingly, the radiation Qss absorbed by the surface layer can be calculated.

In the below ice layer, simple parameterizations based on the Bouguer-Lambert law are used. And the light extinction coefficient κ_i of ice was usually regarded constant during freezing and melting stages. With integration of q_i over the whole ice depth, we can get the Qsi. So the
Qsw=(1−α)Qs−Qss−Qsi can be obtained.

Therefore, coefficients involved in radiative transfer model change through the ice process, so the percentages of the Qss, Qsi, and Qsi were not constant during growth and ablation.

The analyses here are meant for the mean values during the modelling period.
In this study, the down welling solar radiative (incident solar radiation: Qs) flux was observed so the measured value has taken into account the cloud effect. The average Qs = 181W/m^2. The average surface albedo was about 0.42, so the net Qs at ice surface was 106W/m^2.

The solar radiative flux used for surface heat balance Qss was $(1-\alpha)(1-\gamma)Qs$ (Eq 1). The mean value was 47 W/m^2.

The average solar radiative flus penetrated below ice surface layer was 59W/m^2

At ice bottom the penetrating solar radiative flux exponentially decreased to 22W/m^2,

So for ice surface layer Qs = 106-60 = 46W/m^2

For the ice layer Qsi = 59 -22 = 37W/m^2

At ice bottom Qsw = 22W/m^2

So the average percentage =

Qss: 47/106 = 43%

Qsw: 36/106 = 35.8% =~36%

Qsi: 22/106 = 20.75% = ~ 21%

We have added short information on the above description to the *section 2.3*.

L395 During melting period, the lake water temperature below lake ice will increase fast owing to the strong solar radiation. The absorbed solar radiation by ice and the warm temperature should not be ignored for the ice melting. Will the model simulate the lake water temperature? If yes, how about the precision?

The absorbed solar radiation by ice and water were not ignored during ice melting.

The absorption by ice is used to increase the ice temperature and to generate internal melting, and these processes were included in our simulations.

The absorption by under-ice water is used to increase the water temperature and also partly to increase (in turn) the water-to-ice heat flux that mainly caused ice melt from the bottom.

Our model does not simulate the water temperature, but rather uses it as a boundary condition.

L335-L339 According to the manuscript, the monthly mean Ts was consistently lower than the monthly Ta from December through April, while Ts was higher than Ta in November when the ice was rapidly growing, especially when the ice thickness was less than _ 10 cm. But in Table 3, the direction of Qh may not match it?

In this study, the positive flux was defined towards the ice layer. We have clarified this in the revised manuscript.

L405-407 Make sure if the lake (ice) released heat to the atmosphere through the whole ice-covered season with a consistent stable ABL.

For most of the time, the ice surface temperature was lower than the near-surface air temperature indicating a stable atmospheric boundary layer (ABL). Therefore, the atmosphere provided heat to the ice cover through a downward turbulent sensible heat flux (positive Qh in Table 3). However, the total amount of latent heat flux and net long-wave radiative flux (cooling) was large (negative) and exceeded the total amount of net solar radiative flux and sensible heat flux Qh, resulting in heat loss from the ice surface to the atmosphere. And this heat loss resulted in ice gowth.

L424 and Table 1 Lake ice albedo is very important for the simulated results and it may be very low in the plateau as mentioned by authors. But we couldn't get the specific information about your lake ice albedo. How to treat it in the work?

We have applied a sophisticated surface albedo scheme taking into account temperature, snow and ice thickness, solar zenith angle, and atmospheric properties, and distinguishing between visible and near-infrared albedos values (Briegleb et al., 2004). The calculated surface albedo was strongly associated with observed changes in ice thickness, suggesting that the parameterization worked well.

Other changes:

(1) We improved the English readability by a native speaker, many definite/indefinite articles, singular/plural nouns, simple phrases, and sentence patterns have been modified, but are not shown in this response letter.

(2) Julian dates have been removed and replaced by calendar in the text and in all figures.

(3) All "2010/2011" have been reformed to "2010–2011".

(4) Lines 98-101 (and references therein) were removed since it is not essential to the topics.

(5) Line 105: delete "with a stable water level through the year", and "fresh" → brackish".

(6) Line 106-107: delete "Submerged plants grow abundantly in the lake sediment throughout the year.", since it is not essential to the topics.

References listed in the above responses:

Briegleb, B., Bitz, C.M., Hunke, E.C., Lipscomb, W.H., Holland, M.M., Schramm, J., and Moritz, R.: Scientific description of the sea ice component in the Community Climate System Model, Ver. 3, NCAR/TN-463+STR, NCAR Tech Note, 1-78, 2004.

Huang, W., Li, R., Han, H., Niu, F., Wu, Q., and Wang, W.: Ice processes and surface ablation in a shallow thermokarst lake in the central Qinghai-Tibet Plateau, Ann. Glaciol., 57(71), 20-28, 2016.

Launiainen, J.: Derivation of the relationship between the Obukhov stability parameter and the bulk Richardson number for the flux-profile studies. Boundary-Layer Meteorol. 76: 165-179, 1995.

Launiainen, J., Cheng, B.: A simple non-it-erative algorithm for calculating turbulent bulk fluxes in diabatic conditions over water, snow/ice and ground surface. Report Series in Geophysics, 33, Dept. of Geophysics, University of Helsinki. 12 pp, 1995.

Launiainen, J., Cheng, B.: Modelling of ice thermodynamics in natural water bodies. Cold Reg. Sci. Technol., 27, 153-178, 1998.

Lei, Y., Yao, T., Yang, K., Sheng, Y., Kleinherenbrink, M., Yi, S., Bird, B. W., Zhang, X., Zhu, L., and Zhang. G.: Lake seasonality across the Tibet Plateau and their varying relationship with regional mass balance and local hydrology, Geophys. Res. Lett., 44, 892-900, doi: 10.1002/2016GL072062, 2017.

Li, X., Ma, Y., Huang, Y., Hu, X., Wu, X., Wang, P., Li, G., Zhang, S., Wu, H., Jiang, Z., Cui, B., and Liu, L.: Evaporation and surface energy budget over the largest high-altitude saline lake on the Qinghai-Tibet Plateau, J. Geophys. Res.- Atmos., 121(18), 10470-10485, 2016a.

Li, Y., Zhang, C., and Wang, Y.: The verification of millennial-scale monsoon water vapor transport channel in northwest China, J. Hydrol., 536, 273-283, 2016.

Li, Z., Lyu, S., Zhao, L., Wen, L., Ao, Y., and Wang, S.: Turbulent transfer coefficient and roughness length in a high-altitude lake, Tibetan Plateau, Theor. Appl. Climatol., 124, 723-735, 2016.

Lin, Z.J., Niu, F.J., Fang, J.H., Luo, J., and Yin, G.A.: Interannual variations in the hydrothermal regime around a thermokarst lake in Beiluhe, Qinghai-Tibet Plateau, Geomorphology, 276, 16-26, 2017.

Pan, X., Yu, Q., You, Y., Chun, K. P., Shi, X., and Li, Y.: Contribution of supra-permafrost discharge to thermokarst lake water balances on the northeastern Qinghai-Tibet Plateau, J. Hydrol., 555, 621-630, 2017.

Wang, B., Ma, Y., Chen, X., Ma, W., Su, Z., and Menenti, M.: Observation and simulation of lake-air heat and water transfer processes in a high-altitude shallow lake on the Tibetan Plateau, J. Geophys. Res., 120, 12327-12344, 2015.

Modeling experiments on seasonal lake ice mass and energy balance in Qinghai-Tibet Plateau: A case study

Wenfeng Huang[1,2], Bin Cheng[3], Jinrong Zhang[1,2], Zheng Zhang[1,2], Timo Vihma[3], Zhijun Li[4,5], Fujun Niu[5]

[1] Key Laboratory of Subsurface Hydrology and Ecological Effects in Arid Region (the Ministry of Education), Chang'an University, Xi'an 710054, China

[2] School of Environmental Science and Engineering, Chang'an University, Xi'an 710054, China

[3] Finnish Meteorological Institute, Helsinki, Finland

[4] State Key Laboratory of Coastal and Offshore Engineering, Dalian University of Technology, Dalian 116024, China

[5] State Key Laboratory of Frozen Soil Engineering, Northwest Institute of Eco-Environment and Resources, Chinses Academy of Sciences, Lanzhou 730000, China

Correspondence to: Wenfeng Huang (huangwenfeng@chd.edu.cn)

Abstract. The lake-rich Qinghai-Tibet Plateau (QTP) has significant impacts on regional and global water cycles and monsoon systems through heat and water vapor exchange. The lake-atmosphere interactions have been quantified over open-water periods, yet little is known about the lake ice thermodynamics and heat and mass balance during the ice-covered season due to a lack of field data. In this study, a high-resolution thermodynamic ice model was applied in experiments of lake ice evolution and energy balance of a shallow lake in QTP. Basal growth and melt dominated the seasonal evolution of lake ice, but also surface sublimation was crucial for ice loss, accounting for up to 40% of the maximum ice thickness. Sublimation was also responsible for 41% of the lake water loss during the ice-covered period. Simulation results matched the observations well with respect to ice mass balance components, ice thickness, and ice temperature. Strong solar radiation, negative air temperature, low air moisture, and prevailing strong winds were the major driving forces controlling the seasonal ice mass balance. The energy balance was estimated at the ice surface and bottom, and within the ice interior and under-ice water. Particularly, almost all heat fluxes showed significant diurnal variations including incoming, absorbed, and penetrated solar radiation, long-wave radiation, turbulent air-ice heat fluxes, and basal ice-water heat fluxes. The calculated ice surface temperature indicated that the atmospheric boundary layer stratification was consistently stable or neutral throughout the ice-covered period. The turbulent air-ice heat fluxes and the net heat gain by the lake were much lower than those during the open-water period.

1. Introduction

The Qinghai-Tibet Plateau (QTP), characterized by a mean altitude of more than 4000 m above sea level (*asl*) and predominated by a freezing climate, is often referred to as the "Third Pole of the Earth". It harbors thousands of lakes covering a total area of approximately 40,700 km^2 (1.4% of the QTP area) and occupying approximately 50% of lakes located in China (Zhang et al., 2014). The QTP is also a headwater region of major Asian rivers including Yangtze, Yellow, Yarlung Tsangpo (Brahmaputra), Mekong, Salween, and Indus Rivers (Immerzeel et al., 2010). Due to its unique climatic environment (e.g. low air pressure and humidity, intense solar radiation, prevailing strong winds, widespread permafrost and glaciers, and dense lake/river network), QTP directly affects the regional and global water cycle, monsoon system, and atmospheric circulations (Wu et al., 2015; Li et al., 2016b; Su et al., 2016).

The lakes and ponds in QTP play an crucial role in the surface and subsurface hydrological processes (Pan et al., 2014), moisture and heat budgets (Wang et al., 2015; Li et al., 2016a, c; Wen et al., 2016), regional precipitation (Wen et al., 2015), engineering construction (Niu et al., 2011), and gas emission (Wu et al., 2014). The number and surface area of the lakes varies inter-annually. The variations of size are probably due to warming and degradation of permafrost affected by the climate warming through, e.g. thermokarst (Niu et al., 2011), glacier retreating (Liao et al., 2013), increase of precipitation (Lei et al., 2013; Zhang et al., 2014) and strong surface evaporation.

Despite the harsh climatic conditions and the difficulties in access to these lakes, some field campaigns have been performed during ice-free periods in recent years. An unstable or near-neutral atmospheric boundary layer (ABL) prevails over the QTP lake surface in summer (Wang et al., 2015; Li et al., 2015, 2016c). The turbulent heat fluxes show a strong seasonal variation and lag by 2–3 months behind net solar radiation (Li et al., 2016a; Wen et al., 2016). Heat flux dynamics over lake surface differ remarkably from those over other land surface types (like dry/wet grassland) (Biermann et al., 2014). However, the thermal regimes of lakes in QTP and their impacts on the atmosphere boundary layer and surrounding permafrost during wintertime (ice-covered season) remain unclear. Because of sparse field observations, there is an increasing need of models and parameterizations to better understand the lake-air interaction and lake thermal regime (Kirillin et al., 2017; Wang et al., 2015; Wen et al., 2015).

Generally, the QTP lakes and ponds are ice-covered for 3–7 months, depending on their surface area, altitude, and regional climate (Kropáček et al., 2013). Lake ice thermodynamics (ice thickness and temperature) and phenology (the time of freeze-up and break-up, and the duration of the ice cover) play an important role in lake-air interaction (Li et al., 2016a), lake-effect snowfall (Wright et al., 2013), wintertime lake water quality and ecosystems (Kirillin et al., 2012), gas effluxes (Wu et al., 2014), and on-ice transport and operation. All of these issues highlight the accurate representation of QTP lake ice processes. A few investigations on QTP lake ice have been conducted using field measurements and model simulations. Huang et al. (2012, 2013, 2016) reported the ice processes, interior structure, and thermal property in a small shallow thermokarst lake based on their *in situ* observations, and provided significant insights into lake ice thermodynamics and its role in local heat and vapor fluxes and lake water budget. Further, moderate- to high-resolution remote sensing techniques and products, such as MODIS and ENVISAT-ASAR, have been found to be promising and convenient tools for large-scale QTP lake ice research (Kropáček et al., 2013; Tian et al., 2015).

Thermodynamic modeling is an effective and robust methodology to understand lake ice processes and their relationship with local meteorological and hydrological conditions in polar, boreal and temperate regions (Cheng et al., 2014; Semmler et al., 2012; Yang et al., 2012 and 2013).

In this study, we perform a modeling case study of a shallow lake located in the central QTP. Our objectives are (1) to identify the major driving forces that control the seasonal ice mass balance in QTP thermokarst lakes; (2) to quantify the components of mass and energy balance from the ice surface to bottom; (3) to estimate the lake-atmosphere heat and water vapor fluxes through the entire ice-covered period. To the best of our knowledge, lake ice thermodynamic modeling in QTP has not been carried out before. We expect our work can provide a basis for further in situ measurements and upscaling of lake ice simulations over the QTP.

2. Methodology

2.1 Site description

The Beiluhe Basin is located in high pluvial and alluvial plain of the central QTP, with an elevation of 4500–4600 m *asl* (Fig. 1). The topography is undulating, covered by sparse vegetation and sand dunes. This basin is underlain by continuous permafrost 50-80m thick with the volumetric ice content of 30%–50% (Lin et al., 2017). During years 2004-2014, the annual mean air temperature ranged between –4.1 ℃ and –2.9 ℃, and the annual mean ground temperature between –1.8 ℃ and –0.5 ℃(Lin et al., 2017). The annual mean precipitation ranged from 229 to 467 mm (average: 353 mm), while the annual mean potential evaporation ranged from 1588 to 1626 mm (average: 1613 mm) (Lin et al., 2017). There are more than 1200 lakes and ponds with the surface area larger than 1000 m^2 in the Beiluhe Basin. Lake depths are typically 0.5–2.5 m and the shapes are elliptical or elongated.

Lake BLH-A (unofficial name) is located at 34°49.5′N, 92°55.4′E in Beiluhe Basin 4,600 m above sea level. The lake is perennially closed without rivers or streams flowing into and out of it. The minimum and maximum horizontal dimensions of the lake are 120 m and 150 m, respectively, making a total surface area of about 15,000 m^2. The maximum depth is 2.5 m. The water is brackish and has a total dissolved solid of 1.30 g L^{-1}. The lake has been investigated using in situ instrumentation and numerical modeling with respect to lake ice physics (Huang et al., 2011, 2016), hydrothermal regime (Lin et al., 2011), bank retrogression (Niu et al., 2011), and heat intrusion from the lake water to surrounding permafrost (Lin et al., 2017). Considering physical properties of lake ice, a large number of gas bubbles have been found from the top layer of the ice cover. The large gas content caused a small bulk ice density (880–910 kg m^{-3}) and a small thermal conductivity (1.60–2.10 W m^{-1} K^{-1})) (Huang et al., 2012, 2013; Shi et al., 2014).

2.2 Field observations

Field campaigns were conducted in Lake BLH-A through three consecutive winters from 2010–2011 to 2012–2013, to record the ice-water-sediment temperatures (T_i, T_w, and T_{sed}), air temperature (T_a), and surface and bottom growth and decay of the ice cover. A floater was designed and deployed onto the water surface (Fig. 1). A thermistor cable was fixed to the floater to measure the ice-water temperature at 5 cm interval. An upward-looking ultrasonic sensor was also fixed to the floater and positioned at 100 cm depth to monitor depth of the ice-water interface. A downward-looking ultrasonic sensor was fixed to a steel pipe, which had been inserted into the lake sediment by ~60 m, to monitor the position/depth of ice surface. All measures were recorded every 30 min through the whole ice season. The data yielded the following information: the dates of freeze-up and break-up (D_f and D_b) and time series of the vertical positions of (a) the ice-water interface (H_b), representing the basal melt or growth, and (b) the air-ice interface (H_s), representing the surface sublimation or/and melting. Hence, the evolution of ice thickness ($H = H_b - H_s$) was detected. For detailed information on instrumentation, see Huang et al. (2016).

The Beiluhe weather station (BWS), located 800 m southeast from the lake, monitored the air temperature (T_a), air relative humidity (*Rh*), atmospheric pressure (P_a), water vapor pressure in the air (e_a), wind speed (V_a) and direction, incident short- and long-wave irradiance (Q_l and Q_s) at 2 m and 10 m above the ground surface, and accumulated precipitation (water equivalent, *Prec*). In this paper we focus on the ice season of 2010–2011, when the observed datasets have the highest quality and least missing values. Furthermore, the data reveal a typical seasonal cycle of the lake ice phenology (Fig. 2).

In early freezing season in late October, a thin ice layer typically formed at nights and melted during daytime. Finally, a stable ice cover formed in early November (freeze-up). A strong surface sublimation process at the ice-air interface was observed through the whole ice season, reducing the total ice thickness congealed from the ice-water interface. The absolute thickness reached its maximum (~ 60 cm) in early February. On the basis of our field visits during freezing (early December) and melting (late March) stages and the constant low temperature and strong wind through the ice season, we concluded that the bare ice surface was most probably persistently dry without melt water throughout the 2010–2011 ice season.

2.3 Thermodynamic snow and ice model

A well calibrated (Launiainen and Cheng, 1998, Vihma et al., 2002) and widely used (Cheng et al., 2006, 2008; Semmler et al., 2012; Yang et al., 2012 and 2013; Cheng et al., 2014) thermodynamic snow and ice model (HIGHTSI) is applied in this study to investigate Lake BLH surface energy and ice mass balances. The surface heat balance reads:

$$(1-\alpha)(1-\gamma)Q_s + Q_l + \varepsilon\sigma T_s^4 + Q_{le} + Q_h + Q_p + F_c = F_m \qquad (1)$$

where Q_s and Q_l is the incident shortwave and longwave radiation, respectively, α is the surface albedo, γ is the fraction of solar radiation penetrating the surface, ε is the thermal emissivity of the surface (ice/snow), σ is the Stefan-Boltzmann constant, T_s is the surface temperature, Q_{le} and Q_h are the latent and sensible heat fluxes, Q_p is the heat flux from precipitation, which can be neglected in QTP during wintertime, F_c is the conductive heat flux in the ice at the surface, and F_m is the surface heat balance. Heat flux towards the ice surface was defined positive. Surface melting is accordingly calculated as:

$$\rho_i L_f \frac{dH}{dt} + F_m = k_{iup}\frac{\partial T}{\partial z} \qquad (2)$$

where ρ_i is the ice density, L_f is the latent heat of freezing, k_{iup} is the thermal conductivity of ice at upper ice layer, T is the ice temperature, and z is the vertical coordinate. The incident short- and longwave radiative fluxes are either parameterized, taking into account cloudiness, or prescribed by observations or NWP model output. The penetration of solar radiation into the snow and ice is parameterized according to surface albedo and optical properties of snow and ice. The turbulent heat fluxes (Q_e and Q_c) at ice-air interface are parameterized using the bulk-aerodynamic formulae as follows:

$$Q_{le} = \rho_a L C_e V_a (q_s - q_a) \qquad (3)$$

$$Q_h = \rho_a c_p C_h V_a (T_s - T_a) \qquad (4)$$

where ρ_a is the air density, L is the latent heat of sublimation of ice when $T_s < 0$ ℃ or of evaporation of water when $T_s \geq 0$ ℃, V_a is the wind speed at the reference height (2.0 m), T_s is the ice surface temperature, q_s is the saturation specific humidity corresponding to T_s, and q_a and T_a are the specific humidity and temperature of air at the reference height, and C_e and C_h are the bulk transfer coefficients for heat and water vapor, respectively. Both transfer coefficients are parameterized taking into account the thermal stratification of the atmospheric boundary layer (Launiainen and Cheng, 1998; Wang et al., 2015). In addition, Q_{le}/L gives the equivalent thickness of sublimated ice or of evaporated water E.

$$E = \frac{Q_{le}}{L} \qquad (5)$$

Within the ice column, a sophisticated two-layer radiative transfer model is used taking into account a thin surface layer that is different from the ice layer below with respect to optical properties (Maykut and Perovich, 1987).

At the bottom boundary, the ice growth/melt is calculated on the basis of the difference between the heat flux from lake water to ice base (F_w) and the conductive heat flux at the ice bottom layer:

$$\rho_i L_f \frac{dH}{dt} + F_w = k_{idn} \frac{\partial T}{\partial z} \qquad (6)$$

where k_{idn} is the thermal conductivity of ice at ice bottom layer. In HIGHTSI, F_w is either prescribed as a constant value or prescribed based on in situ observations.

The evolutions of thickness and temperature of snow and ice are obtained by solving the heat conduction equations for multiple ice and snow layers. Eq (1) solves the surface temperature, which is used as the upper boundary condition as well as to determine whether surface melting occurs. The ice bottom temperature keeps at the freezing point.

2.4 Meteorological data and model parameters

The meteorological data are based on the BWS (Fig. 3). The 2-m air temperatures observed on the lake site were highly correlated with the measurement at BWS station with averaged difference of 0.3 ℃ (R^2 = 0.98). The T_a has a strong diurnal cycle in response to the large diurnal cycle of solar radiation. The mean T_a was -10.6 ℃ during simulation period from 9 November, 2010, to 25 April, 2011. The northwest winds prevailed during the winter season. The gust wind speed was frequently stronger than 10 m/s. The average wind speed was 6.5 m s^{-1} associated with an average relative humidity of 34 % only.

The daily insolation lasted for 10-12 hours and the average daily (24 h) solar radiation *Qs* was about 390 W m^{-2} during the simulation period, with the daily maximum ranging from 570 to 1140 W m^{-2}. The averaged downward longwave radiation during daytime (8:00-19:00, local time) and nighttime (19:00-8:00) was approximately 177 and 180 W m^{-2}, respectively. The radiative cooling due to negative net radiation was strong during nighttime.

The snow pack was very thin, literally zero, during winter 2010–2011. There were a few minor snowfall events, but no snow accumulation because of strong wind. A major detectable snowfall occurred in early April (~ 9 cm of snow), but the snow was blown off in a short time. For simplicity, snow was not taken into account in the model simulation. The transparent ice allowed solar radiation to penetrate into the ice interior and further down to the under-ice water column, heating the ice/water column daily.

The sky was persistently clear over the whole ice season 2010–2011. High cloudiness and overcast conditions occurred only during late ice season. A slight thin film of fine sand accumulated on the ice surface in early spring coloring the ice surface light yellow. The surface albedo may have accordingly reduced, leading more solar radiation absorption at and below the surface. An albedo parameterization scheme for a climate system model developed by Briegleb et al., (2004) was applied in this study, but the impact of the surface dust film was not taken into consideration.

When running the HIGHTSI model, we have to input values of the heat flux F_w. which is challenging to be observed. Actually, we estimate F_w using heat residual method at ice base based on *in situ* measurements of in-ice temperature profile and the rate of basal ice growth (Huang et al., 2019). But for a reference run, a prescribed time series for the derived F_w was used. The average F_w was approximated 27 W m^{-2}.

For the reference run, model forcing data and parameters are given in Table 1.

3. Results and analysis

3.1 Lake ice thickness and mass balance

The BLH-A lake ice congelation lasted from early November to the beginning of February. Through February, the ice growth reached a thermal equilibrium stage, and the ice thickness did not change much. From the beginning of March, the ice started to melt, most at the ice bottom and also within the ice interior. Finally, the ice cover disappeared at the end of April. The growth, thermal equilibrium, and melting periods lasted for approximately 87, 30, and 56 days, respectively.

The lake ice mass balance consists of the surface ice sublimation and melting, bottom freezing and melting (Fig. 4a). The ice bottom evolution (congelation ice) dominated the ice growth to 0.75 m until day 430 before a melting started at the ice bottom. The model calculated a total surface melting (~0.12 m) at the end of the ice season. A strong loss of latent heat flux during the entire period generated some 0.23 m of lake ice sublimation at the ice surface. The observed air-ice interface evolution (Fig. 2) revealed the integrated impacts of surface sublimation and melting (during the late season), which could not be instrumentally delineated from each other. By regrouping the modeled ice mass balance components, we can calculate the evolution of the ice surface (i.e. surface sublimation + melting) and ice bottom, and compare them with the measurements (Fig. 4b). Although the modeled ice bottom depth is 4.2 cm larger than measured one (Table 2), the HIGHTSI model very well captured the general evolution both at the ice surface and bottom. The modeled total ice thickness (i.e. $Depth_B$–$Depth_S$) is in good agreement with the observations (Fig. 4c). However, during day 460, the ice melting was stopped due to a snowfall event. This short-term pause was not revealed by the model since the snow thickness was assumed zero.

HIGHTSI modeling also affirmed that there are obvious and strong diurnal cycles of freezing and melting at the ice bottom when the ice thickness is less than ~ 20 cm, especially in late spring. For instance, during the melting stage, the ice melts rapidly from 9:00-10:00 to 17:00-18:00, and undergoes an equilibrium or minor growth from 18:00 to 6:00-8:00, then melts again during daytime at the bottom. Besides, the model also detected diurnal variations in the surface sublimation and melting.

Statistical analysis indicated that the model results and measurements for ice mass balance have a high correlation ($R > 0.97$) and small standard deviations (< 3.6 cm), and match very well in terms of surface and bottom depth evolutions and ice thickness with *MAEs* and *RMSEs* generally lower than 5.5 cm (Table 2).

3.2 Lake ice temperatures

The modeled ice temperature regime (Fig. 5) revealed that there are strong diurnal cycles in ice temperature throughout the ice season, following the large diurnal cycle in air temperature and solar radiation. This is consistent with the observed ice thermal dynamics. The calculated surface temperature of ice was continuously lower than the freezing point, except during daytime in late April, when it revealed some cycles of daytime melting and nighttime freezing at the surface.

The calculated and observed vertical profiles of ice temperature were compared at selected time steps (Fig. 6). The ice temperature was modeled quite well during the ice growth period (Figs. 6a-d). During the equilibrium and melting stages, the observed and modeled temperature discrepancies were larger especially at the surface and bottom parts. This could have resulted from several processes. From the beginning of the equilibrium stage, the solar radiation increased gradually and was absorbed by the thermistor sensors at top layer, leading to higher observed values near the surface during daytime (Fig. 6e). During the melting period, the bottommost part of the ice column underwent fast phase change, and the inter-crystal spaces could be filled with underlying warm water. The sensors near the ice bottom actually detected the integrated temperature of ice and water, thus the observed temperature could be quite close to and even slightly higher than the freezing point (0 ℃) (Figs. 6e,f). On the other hand, the linearly interpolated surface depth is likely to cause errors in determining the true sensor depths within the sublimating ice cover, causing some temperature differences.

3.3 Modeled Energy balance

The lake ice thickening and thinning and temperature regime (i.e. phase transitions) are governed by the energy transport and translation through the air-ice-water column. The good performances of HIGHTSI model in calculating the ice mass balance and temperature dynamics argue comprehensive estimates of heat/radiation transfer and partitioning within the air-ice-water column. For a seasonal cycle, the monthly means of various heat fluxes were calculated at the ice surface, within the ice interior, and at the ice bottom (Table 3).

The net shortwave radiation (Q_{sn}) absorbed by the lake acted as a main energy source for ice and water thermodynamics, and followed the seasonal variation of total incident solar radiation (Q_s). The Q_{sn} penetrated through the ice surface and interior, and into the under-ice water column. Therefore, it was divided into three parts: the net solar radiation used for surface energy balance ($Q_{ss}=(1-\alpha)(1-\gamma)Q_s$) (~43% of Q_{sn}), the absorption by the ice interior beneath surface (Q_{si}) (~36%), and the absorption by water (Q_{sw}) (~21%), all of which also showed similar seasonal variation to Q_s. The water heat flux into ice (F_w) that represents the temperature difference between the water and ice bottom, was larger when the ice was thinner. The turbulent heat fluxes did not show strong seasonal variations through the ice season. Furthermore, almost all of the heat fluxes showed strong diurnal variations (Fig. 7). All radiative fluxes (Q_s, Q_{sn}, Q_{si}, and Q_{sw}) had synchronous diurnal cycles, peaked at noon and disappeared through night. The sensible heat flux (Q_h) peaked in the afternoon and had its minimum just before the dawn. The latent heat flux (Q_{le}) had an opposite diurnal pattern with a minimum in the afternoon and maximum in the early morning. The net longwave radiation (Q_{ln}) and surface conductive heat flux (F_c) had roughly opposite diurnal cycles with extremes at midnight.

For the thin surface layer, the upward conductive heat flux (F_c) represents the near surface ice temperature gradient. When the ice was thin (e.g. in November), the larger F_c indicates more heat lost from the ice bottom to surface, and thus rapid ice growth. The net long-wave radiation ($Q_{ln}=Q_l-\varepsilon\sigma T_s^4$) was consistently negative and indicated that the ice surface emitted the heat back to the air/space all the time. The sensible heat flux (Q_h) was generally positive, thus argued heat gain from the air. The large negative latent heat flux (Q_{le}) (Table 3) manifested that the surface sublimation was strong (Fig. 4a). According to the surface heat balance (Eq. 1), the residual F_m was close to zero, indicating a dry cold surface. However, in April, its positive value revealed that the ice melted at surface (Fig. 4a), and the latent heat was induced by evaporation of meltwater during late melting season instead of sublimation of ice.

Within the ice interior, the absorbed solar radiation Q_{si} was used to heat the ice during daytime and thus caused the diurnal variation in ice temperature (Fig. 5), and also led to interior melt in a manner of gas pore expansion during the late ice season (Leppäranta et al., 2010).

Beneath the ice bottom, the under-ice water column absorbed the transmitted solar radiation Q_{sw} and raised its temperature at daytime. According to the lake sediment temperature measurements in BLH-A by Lin et al. (2011, 2017), through the whole ice-covered season the bottom sediment releases quite limited heat to lake water (– 0.2~ –0.6 W m^{-2}), consequently, this heat flux can be ignored. For the energy balance of under-ice water, the penetrated solar radiation is the pivotal heat source, of which 56% is released into the ice bottom (F_w), 44% is used to increase the bulk water temperature and partly is transformed to turbulent kinetic energy forcing water convection, and few (< 0.1%) is transported to bottom sediment (permafrost and talik).

3.4 Model experiment on F_w

Usually, the water-to-ice heat flux F_w is assumed to be constant throughout an ice season when simulating ice thickness in Arctic or temperate lakes. Therefore, under the same weather forcing condition, a number of model experiments have been performed using a constant F_w (ranging from 0 to 50 W m^{-2} with an interval of 5 W m^{-2}).

During the modeling period, the average ice growth at bottom was 0.49 m with a maximum of about 0.72 m. The average and maximum ice thicknesses were 0.38 m and 0.61 m, respectively. Model experiments indicated that the average F_w cannot be smaller than 15 W m^{-2} because otherwise both average and maximum ice thicknesses would differ a lot from observations (Fig. 8). If average F_w is about 35 W m^{-2}, the modeled average and maximum net total ice thickness are not far from the observed values, but have large offsets at ice bottom, especially for the maximum ice growth at ice bottom. If average F_w is more than 35 W m^{-2}, the errors for both average and maximum ice thicknesses are getting larger. It seems when average F_w is between 20 W m^{-2} and 30 W m^{-2}, the modeled results are within the ranges of observed values with respect to total and bottom growth ice thicknesses.

In reality, F_w is not a constant value. Model experiments argued that the mass balance at ice base cannot be reproduced using constant F_w through the whole ice season. Based on heat residual method, we created the time series of F_w (Fig. 9) to carry out the reference run (Fig. 4) that gave a very good agreement to the observations.

Different from the ocean and large deep lake, where the variation of F_w is largely driven by the under-ice currents (Krishfield and Perovich, 2005; Rizk et al., 2014), BLH-A is very shallow and the water below ice is largely at a standstill, so the driving force for F_w most likely is the penetrated solar radiation. The modeled solar radiative flux that penetrates through the ice layer and reaches at ice bottom is plotted in Fig. 9. In early simulation, ice was very thin and the surface albedo is small, so large part of solar radiation penetrated through ice layer and warmed the underlying water, creating a large F_w. When ice was getting thicker, the surface albedo increased and the penetrated solar radiation was reduced. In later part of the season, melting of ice reduced the surface albedo, the downward solar radiation was simultaneously increased, and more solar radiation was accordingly absorbed in the lake water below the ice. The average solar radiation absorbed by the under-ice water column during the entire simulation period was 22 W m^{-2}. Additionally, the heat flux induced by changes in underlying water temperature (i.e. heat content in water) was estimated to be 3 W m^{-2}. The total 25 W m^{-2} is in the range of good agreement between observed and modeled ice thickness (Fig. 8).

4. Discussion

4.1 Implication on ABL over ice-covered lakes

The characteristics of the ABL play a direct role in the turbulent heat and mass fluxes. The modeled and observed temperature profiles through the air-ice-water column presented here can give a close insight into the features of the ABL over the lake during the ice-covered period taking the temperature difference between the lake (ice) surface and the air as a bulk stability indicator. The ice surface temperature (T_s) was generally lower than the air temperature (T_a). The monthly mean T_s was consistently lower than the monthly T_a by 1.24 ± 0.55 °C from December through April, indicating a persistent stable ABL through the ice-covered period (Fig. 10). However, the T_s was 0.31 °C higher than T_a in November when the ice was rapidly growing, especially when the ice thickness was less than ~ 10 cm (i.e., before Nov. 20).

Previous investigations revealed that the QTP lakes are predominantly characterized by unstable ABL during open-water period (Li et al., 2015; Wang et al., 2015; Wen et al., 2016). The present results indicated that the ABL over lake turns into a stable or neutral stratification soon after the lake ice forms. When the lake ice disappears, the ABL soon turns into an unstable straitfication again (Wen et al., 2016). However, short-term periods of unstable ABL were observed for approximately 25% of the ice duration period. The unstable conditions usually took up on diurnal scale especially following sudden drops of the air temperature.

4.2 The air-lake heat exchange

Diurnal changes in turbulent heat fluxes, however, are large and are commonly seen in high-latitude and high-altitude lakes (e.g. Vesala et al., 2006; Rouse et al., 2008; Nordbo et al., 2011; Wang et al. 2015; Li et al. 2016a, c; Wen et al. 2016). In our study, the mean values of turbulent heat fluxes of Q_h and Q_{le} were 14 W m^{-2} and –41 W m^{-2}, respectively. These numbers are in line with observations that were obtained in QTP lakes in winter season (Li et al., 2016a). At seasonal scale, the Q_h and Q_{le} over lake ice are approximately 40%–60% lower than values during ice-free seasons, demonstrating the role of ice as an insulator. The present turbulent heat fluxes are somewhat larger than those observed at Great Slave Lake (Blanken et al., 2000) and a boreal lake in south Finland (Nordbo et al., 2011) during the open-water period. This is attributed to the stronger wind and drier air prevailing over the QTP.

The net heat exchange ($Q_{net}= Q_{sn} +Q_{ln}+Q_h+Q_{le}$) through the atmosphere-lake interface showed strong diurnal and seasonal cycles. Q_{net} increased gradually through the whole ice season. The lake ice released heat into the atmosphere until early March, and then gained heat from the atmosphere. Integrated over the ice season, the lake released heat of about 266 MJ m^{-2} (i.e. ~17 W m^{-2}).

4.3 Water vapor flux and lake water balance

The water balance in a lake reads

$$\Delta V = P - E + R_s + R_g \qquad (7)$$

where ΔV is the lake water change, and P, E, R_s and R_g are the precipitation, evaporation, net surface inflow and subsurface inflow, respectively.

During the freezing season in central QTP, the precipitation is generally quite small and the surface inflow and outflow through gullies and streams are typically blocked due to the freezing conditions. Therefore, the lake water balance is strongly affected by evaporation/sublimation and subsurface inflow/outflow.

Assuming ice density of 900 kg m^{-3}, the modeled sublimated ice thickness E can be converted to water equivalent (WE) (Fig. 12). The monthly mean sublimation was the weakest in December and January, but higher in February and March. This is probably due to the stronger winds and higher ice surface temperature; the latter was favored by more incident long- and short-wave radiation than before. Through the entire ice season, the ice surface water loss due to evaporation/sublimation was approximately 207 mm *WE*.

The BLH-A lake water level observations revealed a decrease of 0.50 m through the entire ice season (Lin et al., 2017). The surface evaporation/sublimation hence accounts for 41% of lake water loss during the ice-covered period and for 42% of annual water loss (Pan et al., 2017). The remaining part of water loss is probably caused by vertical percolation through the lake sediment to supply deep groundwater, since the talik (a layer of year-round unfrozen ground) beneath the lake has developed through the underlying permafrost (Lin et al., 2011, 2017; Niu et al., 2011), and by the lateral water discharge into ambient soil during the thickening and thinning of frozen active layer (Pan et al., 2017; Lin et al., 2017). But over the entire hydrological year, the lake water loss through subsurface discharge and evaporation/sublimation is roughly offset by the heavy precipitation, surface runoff, and supra-permafrost recharge during warm seasons (Lei et al., 2017; Pan et al., 2017). Therefore, the studied lake level is nearly stabilized inter-annually (Lin et al. 2017; Gao et al., 2018).

5. Summary and conclusions

The ice season was characterized by a freezing period (9 November – 4 February), a thermal equilibrium period (5 February –10 March), and a melting period (11 March – 30 April). During the freezing period, strong atmospheric cooling caused a growth of congelation ice of about 70 cm. The major driving force for ice growth was a consistent subzero air temperature (mean -13 ℃) and a strong average net longwave radiative cooling (-97 W m^{-2}), although the ice surface absorbed a net solar radiative flux of 77 W m^{-2} on the average.

During melting period, the ice melt rate was about 14 mm/day. Basal melting dominated and surface melting was only seen by the very end of the ice season, because air temperatures remained subzero during most of the winter. A total 0.23 m of ice thickness was lost at the surface due to a sustained sublimation process during the entire study period. This was caused by a combined effect of prevailing strong winds and dry air. The observed average wind speed and relative humidity were 7 m s^{-1} and 34%, respectively.

Comparisons with an Arctic lake revealed the uniqueness of QTP lakes especially with respect to the atmospheric forcing, lake geometry, ice cover (free of snow), and under-ice hydro-thermodynamics (Table 4). These features challenge the existing lake ice models that are mainly developed for Arctic and temperate regions. However, present modeling experiments indicated that HIGHTSI could yield reasonable results in terms of the surface and bottom freezing/ablation and ice thermodynamics.

Additionally, HIGHTSI results indicated that the net long-wave radiative cooling (-97 W m^{-2}) and upward conductive heat flux in the ice interior as well as turbulent latent heat flux dominated the ice surface energy and mass balance. The average net solar radiative flux was large (181 W m^{-2}); 40% of it was reflected back to the space, 34% was absorbed below the ice surface, and only 26% was used for surface energy balance. Diurnal cycles of surface heat fluxes were driven by the diurnal variations of shortwave radiation. The observed air temperature and calculated ice surface temperature suggested a consistent stably stratified ABL during most of the ice-covered period, except when the ice thickness was less than ~10 cm. Averaged over the entire ice-covered season, the lake (ice) released 17 W m^{-2} heat to the atmosphere.

The ice surface mass balance was dominated by surface ice sublimation, which was modeled very well. The sublimation was demonstrated to be a key component for lake water balance and accounted for 41% of lake water loss during wintertime. In light of the generally low air humidity and strong wind over QTP, the sublimation can be critical for the water balance of a large number of shallow lakes and ponds over the QTP, and further research (observations and modelling) is needed for quantification of sublimation in a regional scale over QTP.

The water-ice heat flux F_w controlled the basal, and thus, the net ice thickness evolution. The model experiments indicated that constant F_w through the whole ice season cannot produce a reasonable basal mass balance. A parameterized time series of F_w was used and yielded realistic results. This confirmed the temporal variation in F_w in shallow QTP thermokarst lakes. Many more observations should be made to quantify F_w and better understand the physics governing it.

The present modeling experiments indicated that the largest uncertainty for QTP lake ice modeling is the effect of F_w. Thermokarst lakes on QTP are typically shallow and small, without significant surface water input and output, implying that through-lake current or lake-wide circulation under the ice cover are negligible (Kirillin et al., 2015). Cold sediment layer limits the heat release into the overlying water (Lin et al., 2011). However, the solar radiation is strong (due to persistent clear-sky conditions), and the lake ice cover is consistently free of snow. In QTP, the surface albedo of ice in large deep lakes can be unprecedentedly small (<0.2) (Li et al., 2018). Indeed, in our study the Briegleb albedo scheme yielded a small albedo, in particular, when the ice was thin. Intensive penetrative solar radiation can drive under-ice turbulent mixing of mass and heat (Mironov et al., 2002). However, the quantitative effects of penetration of solar radiation on F_w are not yet well known, and new field experiments are needed.

Snow was neglected in this modeling work. However, snowfall occasionally occurs on QTP, and may have a strong impact in ice mass balance, especially for large lakes (Cheng et al., 2014). The major impact of snow on ice thermodynamics is the insulation effect (Leppäranta, 2015). Snow-ice is not likely to form on QTP, since in early winter the air temperature drops fast and the ice freezes quickly. However, superimposed ice may be formed in late spring, if there is thick snow on top of ice. Otherwise, snow can compensate the strong ice mass loss due to sublimation, decreasing the water loss in QTP lakes in winters.

Data availability. The datasets on lake ice temperatures and thickness, and meteorological forcing used for modeling and comparison can be downloaded from https://www.researchgate.net/publication/329826495_QTP_lake_ice_and_meteorology_data. Model code and results are available from the first (huangwenfeng@chd.edu.cn) and second author (Bin.Cheng@fmi.fi) by request.

Competing interests. The authors declare no competing interests.

Acknowledgements. This work is supported by the National Natural Science Foundation of China (41402203, 51579028), the Natural Science Fund of Shaanxi Province (2018JQ4021), the Special Fund for Basic Scientific Research of Central Colleges (310829171002, 310829161006), and the Open Fund of State Key Laboratory of Frozen Soils Engineering (SKLFSE201604). We are also grateful to the staff from the Field Station of Permafrost Engineering and Environmental Tests for their field assistance, and PEEX program for providing international cooperation.

References

Biermann, T., Babel, W., Ma, W., Chen, X., Thiem, E., Ma. Y., and Foken, T.: Turbulent flux observations and modeling over a shallow lake and a wet grassland in the Nam Co basin, Tibetan Plateau, Theor. Appl. Climatol., 116, 301-316, 2014.

Blanken, P.D., Rouse, W.R., Culf, A.D., Spence, C., Boudreau, L.D., Jasper, J.N., Kochtubajda, B., Schertzer, W.M., Marsh, P., and Verseghy, D.: Eddy covariance measurements of evaporation from Great Slave Lake, Northwest Territories, Canada, Water Res. Res., 36(4), 1069-1077, 2000.

Briegleb, B., Bitz, C.M., Hunke, E.C., Lipscomb, W.H., Holland, M.M., Schramm, J., and Moritz, R.: Scientific description of the sea ice component in the Community Climate System Model, Ver. 3, NCAR/TN-463+STR, NCAR Tech Note, 1-78, 2004.

Cheng, B., Vihma, T., Rontu, L., Kontu, A.: Evolution of snow and ice temperature, thickness and energy balance in Lake Orajärvi, northern Finland, Tellus A, 66, 21564, http://dx.doi.org/10.3402/tellusa.v66.21564, 2014.

Cheng, B., Vihma, T., Pirazzini, R., and Granskog, M.: Modeling of superimposed ice formation during spring snowmelt period in the Baltic Sea, Ann. Glaciol., 44, 139–146, 2006.

Cheng, B., Zhang, Z., Vihma, T., Johansson, M., Bian, L., Li, Z., and Wu, H.: Model experiments on snow and ice thermodynamics in the Arctic Ocean with CHINARE 2003 data, J. Geophys. Res., 113, C09020, doi:10.1029/2007JC004654, 2008.

Huang, W., Han, H., Shi, L., Niu, F., Deng, Y., and Li, Z.: Effective thermal conductivity of thermokarst lake in Beiluhe Basin, Qinghai-Tibet Plateau, Cold Reg. Sci. Technol., 85, 34-41, 2013.

Huang, W., Li, R., Han, H., Niu, F., Wu, Q., and Wang, W.: Ice processes and surface ablation in a shallow thermokarst lake in the central Qinghai-Tibet Plateau, Ann. Glaciol., 57(71), 20-28, 2016.

Huang, W., Li, Z., Han, H., Niu, F., Lin, Z., and Leppäranta, M.: Structural analysis of thermokarst lake ice in Beiluhe Basin, Qinghai-Tibet Plateau, Cold Reg. Sci. Technol., 72, 33-42, 2012.

Huang, W., Zhang, J., Leppäranta, M., Li, Z., Cheng, B., and Lin, Z.: Thermal structure and water-ice heat transfer in a shallow ice-covered thermokarst lake in central Qinghai-Tibet Plateau, to be submitted, 2019.

Immerzeel, W.W., van Beek, L.P.H., and Bierkens, M.F.P.: Climate change will affect the Asian water towers, Science, 328, 1382-1385, 2010.

Jonas, T., Terzhevik, A.Y., Mironov, D.V., and Wüest, A.: Radiatively driven convection in an ice-covered lake investigated by using temperature microstructure technique, J. Geophys. Res., 108(C6), 3183, doi: 10.1029/2002JC001316, 2003.

Kirillin, G.B., Forrest, A.L. Graves, K.E., Fischer, A., Engelhardt, C., and Laval, B.E.: Axisymmetric circulation driven by marginal heating in ice-covered lakes, Geophys. Res. Lett., 42, 2893-2900, 2015.

Kirillin, G., Leppäranta, M., Terzhevik, A., Granin, N., Bernhardt, J., Engelhardt, C., Efremova, T., Golosov, S., Palshin, N., Sherstyankin, P., Zdorovennova, G., and Zdorovennov, R.: Physics of seasonally ice-covered lakes: a review, Aquat. Sci., 74(4), 659-682, 2012.

Kirillin, G., Wen, L., and Shatwell, T.: Seasonal thermal regime and climatic trends in lakes of the Tibetan Highlands, Hydrol. Earth Syst. Sci., 21, 1895-1909, 2017.

Krishfield, R.A., and Perovich, D.K.: Spatial and temporal variability of oceanic heat flux to the Arctic ice pack, J. Geophys. Res., 110, C07021, doi: 10.1029/2004JC002293, 2005.

Kropáček, J., Maussion, F., Chen, F., Hoerz, S., and Hochschild, V.: Analysis of ice phenology of lakes on the Tibetan Plateau from MODIS data, The Cryosphere, 7, 287-301, 2013.

Launiainen, J., and Cheng, B.: Modeling of ice thermodynamics in natural water bodies, Cold Reg. Sci. Technol., 27(3), 13-178, 1998.

Lei, Y., Yao, T., Yang, K., Sheng, Y., Kleinherenbrink, M., Yi, S., Bird, B. W., Zhang, X., Zhu, L., and Zhang. G.: Lake seasonality across the Tibet Plateau and their varying relationship with regional mass balance and local hydrology, Geophys. Res. Lett., 44, 892-900, doi: 10.1002/2016GL072062, 2017.

Lei, Y., Yao, T., Bird, B. W., Yang, K., Zhai, J., and Sheng, Y.: Coherent lake growth on the central Tibetan Plateau since the 1970s: Characterization and attribution, J. Hydrol., 483(3), 61-67, 2013.

Leppäranta, M.: Freezing of lakes and the evolution of their ice cover, Springer, Berlin, Heidelberg, 2015.

Leppäranta, M., Terzhevik, A., and Shirasawa, K.: Solar radiation and ice melting in Lake Vendyurskoe, Russian, Hydrol. Res., 41(1), 50-62, 2010.

Li, X., Ma, Y., Huang, Y., Hu, X., Wu, X., Wang, P., Li, G., Zhang, S., Wu, H., Jiang, Z., Cui, B., and Liu, L.: Evaporation and surface energy budget over the largest high-altitude saline lake on the Qinghai-Tibet Plateau, J. Geophys. Res.- Atmos., 121(18), 10470-10485, 2016a.

Li, Y., Zhang, C., and Wang, Y.: The verification of millennial-scale monsoon water vapor transport channel in northwest China, J. Hydrol., 536, 273-283, 2016b.

Li, Z., Ao, Y., Lyu, S., Lang, J., Wen, L., Stepanenko, V., Meng, X., and Zhao, L.: Investigations of the ice surface albedo in the Tibetan Plateau lakes based on the field observation and MODIS products, J. Glaciol., doi: 10.1017/jog.2018.35, 2018.

Li, Z., Lyu, S., Zhao, L., Wen, L., Ao, Y., and Wang, S.: Turbulent transfer coefficient and roughness length in a high-altitude lake, Tibetan Plateau, Theor. Appl. Climatol., 124, 723-735, 2016c.

Li, Z., Lyu, S., Ao, Y., Wen, L., Zhao, L., and Wang, S.: Long-term energy flux and radiation balance observations over Lake Ngoring, Tibetan Plateau, Atmos. Res., 155, 13-25, 2015.

Liao, J., Shen, G., and Li, Y.: Lake variations in response to climate change in the Tibetan Plateau in the past 40 years, Int. J. Digit. Earth, 6(6), 534-549, doi:10.1080/17538947.2012.656290, 2013.

Lin, Z.J., Niu, F.J., Fang, J.H., Luo, J., and Yin, G.A.: Interannual variations in the hydrothermal regime around a thermokarst lake in Beiluhe, Qinghai-Tibet Plateau, Geomorphology, 276, 16-26, 2017.

Lin, Z., Niu, F., Liu, H., and Lu, J.: Hydrothermal processes of alpine tundra lakes, Beiluhe Basin, Qinghai-Tibet Plateau, Cold Reg. Sci. Technol., 65, 446-455, 2011.

Maykut, G. A., and Perovich, D. K., 1987. The role of shortwave radiation in the summer decay of a sea ice cover. J. Geophys. Res. 92(C7), 7032–7044.

Mironov, D., Terzhevik, A., Kirillin, G., Jonas, T., Malm, J. and Farmer, D.: Radiatively driven convection in ice-covered lakes: Observations, scaling, and a mixed layer model, J. Geophys. Res., 107(C4), 3032, doi: 10.1029/2001JC000982, 2002.

Mountain Research Initiative EDW Working Group: Elevation-dependent warming in mountain regions of the world, Nature Clim. Change, 5, 424-430, 2015.

Niu, F., Lin, Z., Liu, H., and Lu, J.: Characteristics of thermokarst lakes and their influence on permafrost in Qinghai-Tibet Plateau, Geomorphology, 132, 222-233, 2011.

Nordbo, A., Launiainen, S., Mammarella, I., Leppäranta, M., Houtari, J., Ojala, A., and Vesala, T.: Long-term energy flux measurements and energy balance over a small boreal lake using eddy covariance technique, J. Geophys. Res., 116, D02119, doi: 10.1029/2010JD014542, 2011.

Pan, X., Yu, Q., You, Y., Chun, K. P., Shi, X., and Li, Y.: Contribution of supra-permafrost discharge to thermokarst lake water balances on the northeastern Qinghai-Tibet Plateau, J. Hydrol., 555, 621-630, 2017.

Rizk, W., Kirillin, G., and Leppäranta, M.: Basin-scale circulation and heat fluxes in ice-covered lakes, Limnol. Oceanogr., 59(2), 445-464, , 2014.

Semmler, T., Cheng, B., Yang, Y., and Rontu, L.: Snow and ice on Bear Lake (Alaska)-sensitivity experiments with two lake ice models, Tellus A, 64, 17339, doi:10.3402/tellusa.v64i0.17339, 2012.

Shi, L., Li, Z., Niu, F., Huang, W., Lu, P., Feng, E., and Han, H.: Thermal diffusivity of thermokarst lake ice in the Beiluhe basin of the Qinghai-Tibet Plateau, Ann. Glaciol., 55(66), 153-158, 2014.

Su, F., Zhang, L., Ou, T., Chen, D., Yao, T., Tong, K., and Qi, Y.: Hydrological response to future climate changes for the major upstream river basins in the Tibetan Plateau, Global Planet. Change, 136, 82-95, 2016.

Tian, B., Li, Z., Engram, M. J., Niu, F., Tang, P., Zou, P., and Xu, J.: Characterizing C-band backscattering from thermokarst lake ice on the Qinghai-Tibet Plateau, ISPRS J. Photogramm. Remote Sens., 104, 63-76, 2015.

Venäläinen, A., Tuomenvirta, H., Pirinen, P., Drebs A.: A Basic Finnish Climate Data Set 1961-2000 – Description and Illustrations. Finnish Meteorological Institute Reports 5, 2005.

Vesala, T., Houtari, J., Rannik, U., Suni, T., Smolander, S., Sogachev, A., Launiainen, S., and Ojala, A.: Eddy covariance measurements of carbon exchange and latent and sensible heat fluxes over a boreal lake for a full open-water period, J. Geophys. Res., 111, D11101, doi: 10.1029/2005JD006365, 2006.

Wang, B., Ma, Y., Chen, X., Ma, W., Su, Z., and Menenti, M.: Observation and simulation of lake-air heat and water transfer processes in a high-altitude shallow lake on the Tibetan Plateau, J. Geophys. Res., 120, 12327-12344, 2015.

Wen, L., Lyu, S., Kirillin, G., Li, Z., and Zhao, L.: Air-lake boundary layer and performance of a simple lake parameterization scheme over the Tibetan highlands, Tellus A, 68, 31091, doi:10.3402/tellusa.v68.31091, 2016.

Wen, L., Lyu, S., Li, Z., Zhao, L., and Nagabhatla, N.: Impacts of the two biggest lakes on local temperature and precipitation in the Yellow River Source Region of the Tibetan Plateau, Adv. Meteorol., 2015, 248031, doi:10.1155/2015/248031, 2015.

Wright, D.M., Posselt, D.J., and Steiner, A.L.: Sensitivity of lake-effect snowfall to lake ice cover and temperature in the Great Lakes region, Mon. Weather Rev., 141, 670-689, 2013.

Wu, G., Duan, A., Liu, Y., Mao, J., Ren, R., Bao, Q., He, B., Liu, B., and Hu, W.: Tibetan Plateau climate dynamics: recent research progress and outlook, Natl. Sci. Rev., 2, 100-116, , 2015.

Wu, Q., Zhang, P., Jiang, G., Yang, Y., Deng, Y., and Wang, X.: Bubble emissions from thermokarst lakes in the Qinghai-Xizang Plateau, Quatern. Int., 321, 65-70, 2014.

Yang, K., Ye, B., Zhou, D., Foken, T., Qin, J., and Zhou, Z.: Response of hydrological cycle to recent climate changes in Tibetan Plateau, Climatic Change, 109, 517-534, 2011.

Yang, Y., Cheng, B., Kourzeneva, E., Semmler, T., Rontu, L., Leppäranta, M., Shirasawa, K., and Li, Z.: Modelling experiments on air–snow–ice interactions over Kilpisjärvi, a lake in northern Finland, Boreal Env. Res., 18(5), 341–358, 2013.

Yang, Y., Leppäranta, M., Cheng, B., Heil, P., Li, Z.: Numerical modeling of snow and ice thickness in Lake Vanajärvesi, Finland, Tellus A, 64, 17202, doi:10.3402/tellusa.v64i0.17202, 2012.

Zhang. G., Yao, T., Xie, H., Zhang, K., and Zhu, F.: Lakes' state and abundance across the Tibetan Plateau, Chinese Sci. Bull., 59(24), 3010-3021, 2014.

Table 1. Parameters and input data applied in the model reference run

Variables	Value	Source
V_a, T_a, Rh, Q_s, Q_l	Time series	Observations at BWS
Ice density ρ_i	900 kg m^{-3}	Huang et al. (2012, 2013)
Thermal conductivity k_i	1.80 W m^{-1} K^{-1}	Huang et al. (2013)
Albedo α	0.1- 0.55	Briegleb et al. (2004)
Ice extinction coefficient κ_i	(1.5–17) m^{-1}	Launiainen and Cheng (1998) adapted from Grenfell and Maykut (1977)
Bottom heat flux F_w	Time series	Parameterized based on in-ice temperature profile and ice bottom growth rate (Huang et al., to be submitted)
Initial ice thickness	0.05 m	Observation
Initial ice temperature	Linear interpolation between T_a and T_b	Calculation

Table 2. The mean bias error (*MBE*), mean absolute error (*MAE*), standard deviation (*STD*), root mean square error (*RMSE*), and correlation coefficient (*R*) between modeled and observed ice mass balance components with *n*=4023 (in cm)

Items	Surface height	Bottom height	Ice thickness
MBE	0.2	4.2	4.1
MAE	2.5	4.8	4.3
STD	2.9	3.6	3.0
RMSE	2.9	5.5	5.0
R	0.97	0.99	0.99

Table 3. The monthly means of heat fluxes (in W m^{-2}) within the air-ice-water column. Q_s: incident solar radiation; Q_{sn}: net solar radiation; Q_{ss}: net solar radiation for surface heat balance; Q_{ln}: net longwave radiation; Q_h: sensible heat flux; Q_{le}: latent heat flux; F_c: surface conductive heat flux; F_m: net surface heat flux, that is, the sum of Q_{ss}, Q_{ln}, Q_h, Q_{le} and F_c; Q_{si}: solar radiation absorption within the ice interior; Q_{sw}: solar radiation into under-ice water; F_w: heat flux from water into ice.

Month	11	12	1	2	3	4
Q_s	162	142	138	176	208	259
Q_{sn}	110	69	63	110	135	169
Q_{ss}	37	30	32	57	65	62
Q_{ln}	-112	-100	-83	-87	-79	-73
Q_h	-10	15	15	17	-1	4
Q_{le}	-46	-31	-32	-54	-53	-53
F_c	125	85	68	68	69	63
F_m	-6	-0.1	0.1	0.2	2	4
Q_{si}	35	26	23	40	49	63
Q_{sw}	39	14	8	14	21	43
F_w	34	21	20	20	21	36

Table 4. Comparisons of lake and meteorological features between Lake BLH-A and an Arctic lake (Lake Orajärvi)

Items	Lake BLH-A	Lake Orajärvi**
Surface area	0.015 km^2	11 km^2
Mean depth	2.5 m	4.4 m
Altitude	4600 m	182 m
Annual precipitation	353 mm	500 mm
Annual evaporation	1613 mm	450 mm (Venäläinen et al., 2005)
Air temperature*	-10.6 ℃	-9~-10 ℃
Wind speed*	6.5 m s^{-1}	2.3 m s^{-1}
Relative humidity*	34%	85%~87%
Short-wave radiation*	390 W m^{-2}	41-46 W m^{-2}
Long-wave radiation*	180 W m^{-2}	240-260 W m^{-2}
Net long-wave radiation*	-89 W m^{-2}	-19~-27 W m^{-2}
Snow cover	Negligible (light dust)	Up to over 30 cm
Ice surface sublimation	30 cm	Negligible
Ice structure	Congelation ice	Snow-ice + superimposed ice + congelation ice

*averaged over whole ice season

**data during winters of 2010-2012 were used for statistics

Figure 1. Location of Lake BLH-A. The lower left insert photo shows the lake ice cover including numerous large bubbles, while the lower right insert shows field instrumentation for temperature and ice thickness measurements. Thin deposited find sand film (dark yellow) is also seen in both inserts.

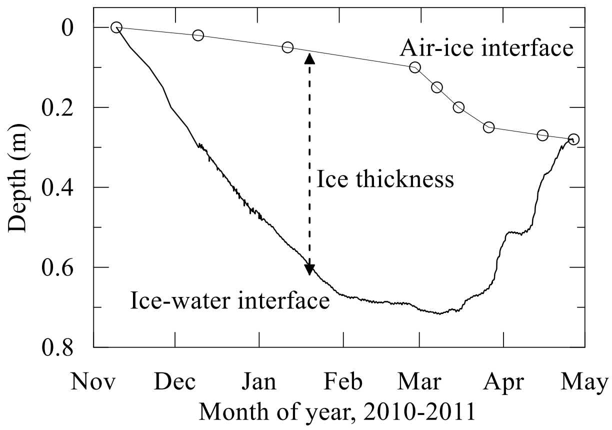

Figure 2. The observed lake ice thickness evolution over the whole 2010–2011 ice season. The open circles denote the observed location of the ice surface, and the solid lines connecting the circles denote the linear interpolation.

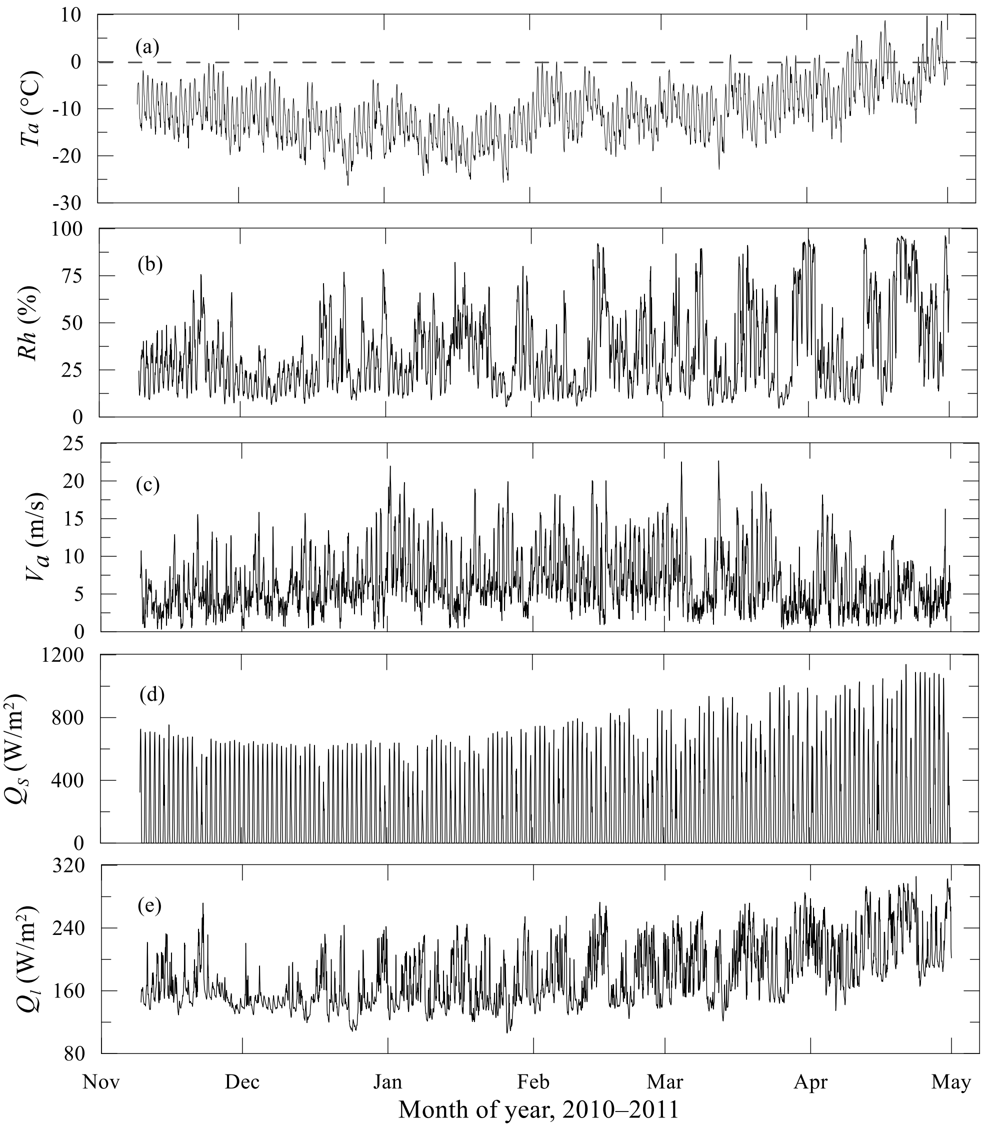

Figure 3. The time series of observed meteorological variables through the whole ice season of 2010–2011. (a) daily mean air temperature T_a, (b) relative humidity *Rh*, (c) wind speed V_a, (d) incident shortwave solar radiation Q_s, and (e) incident longwave radiation Q_l.

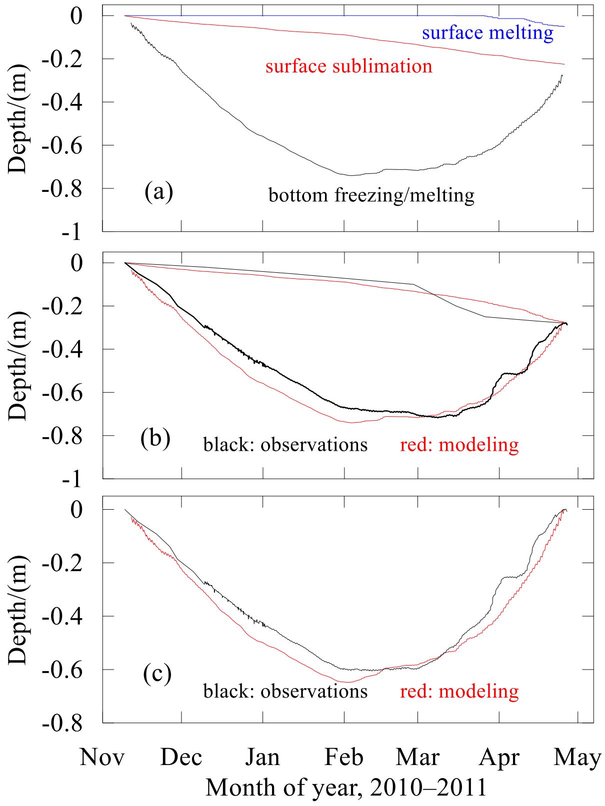

Figure 4. The HIGHTSI modeled BLH lake ice mass balance components (a), the ice surface and bottom evolution (b), and the ice thickness (c).

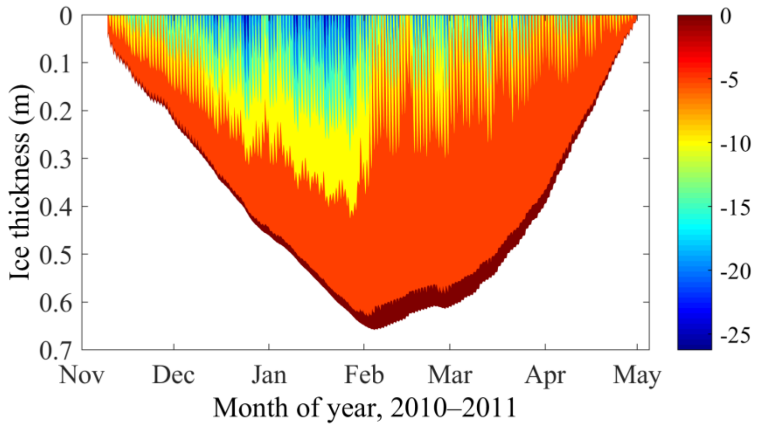

Figure 5. HIGHTSI modeled ice temperature regime for winter 2010–2011.

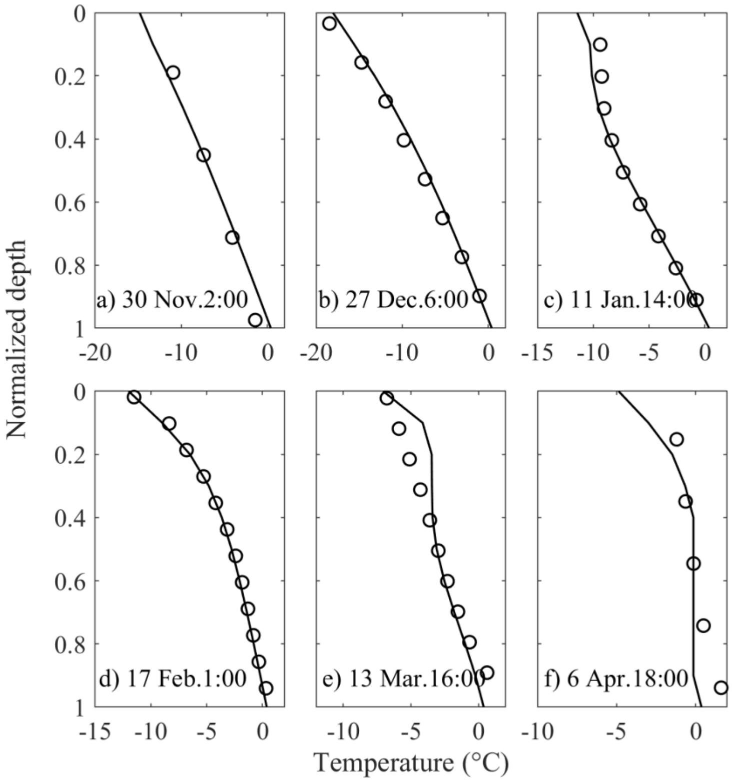

Figure 6. Comparisons of modeled (lines) and observed (circles) vertical temperature profiles of within ice at selected time steps. A normalized depth (depth divided by ice thickness) is used as the y-axis (0 and 1 denote the ice surface and bottom, respectively).

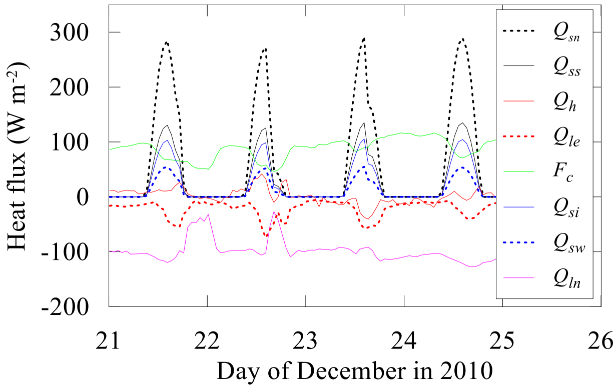

Figure 7. Diurnal patterns of various radiation/heat fluxes

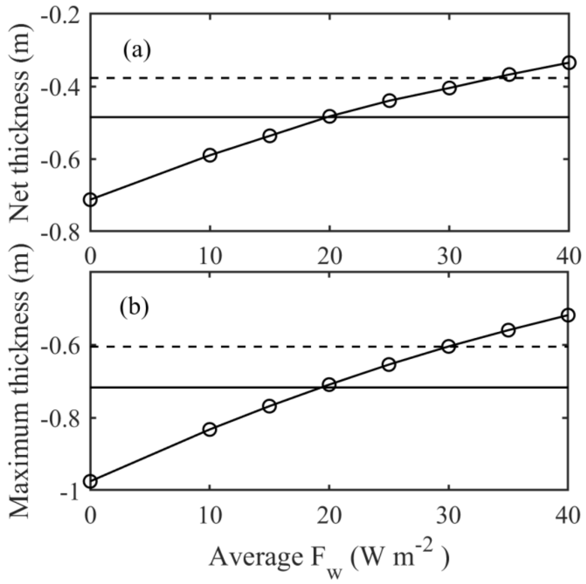

Figure 8. Modeled (lines with circles) average (a) and maximum (b) ice thickness applying different constant F_w. The broken lines are observed average and maximum ice thickness during the simulation period. The solid lines are observed average and maximum ice growth at ice bottom.

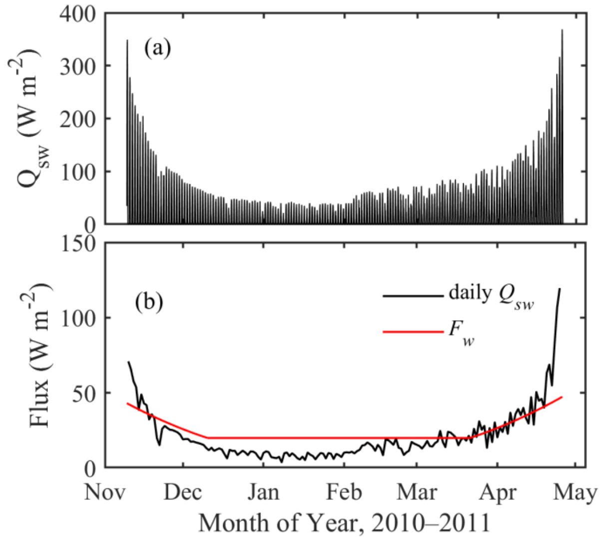

Figure 9. Modeled solar radiation penetration (Q_{sw}) into the under-ice water column: hourly (a) and daily averages (b) with prescribed F_w during the simulation period.

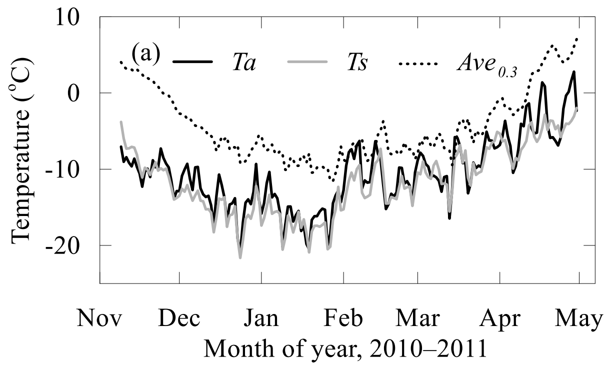

Figure 10. Daily means of the observed air temperature (T_a), the averaged ice/water temperature of the top 30 cm ($Ave_{0\text{-}0.3}$), and the calculated ice surface temperature (T_s).

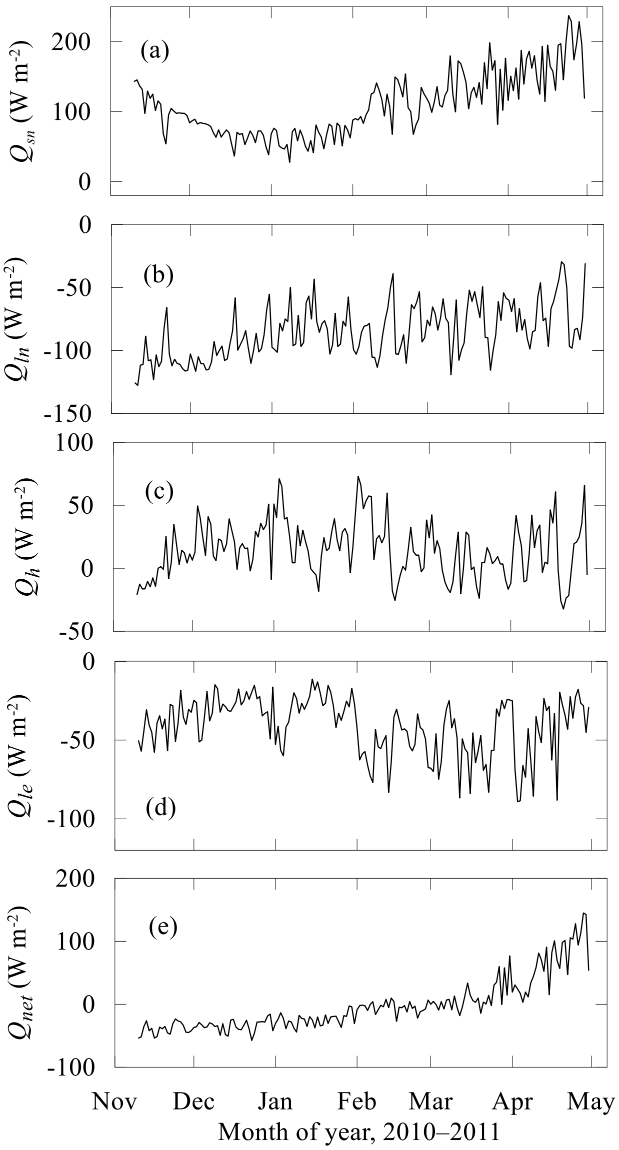

Figure 11. Daily means of the surface energy balance components of net shortwave (Q_{sn}) and longwave (Q_{ln}) radiation, turbulent sensible (Q_h) and latent (Q_e) heat fluxes, and net flux into the lake (Q_{net}= Q_{sn}+Q_{ln}+Q_h+Q_{le}) though the entire ice season.

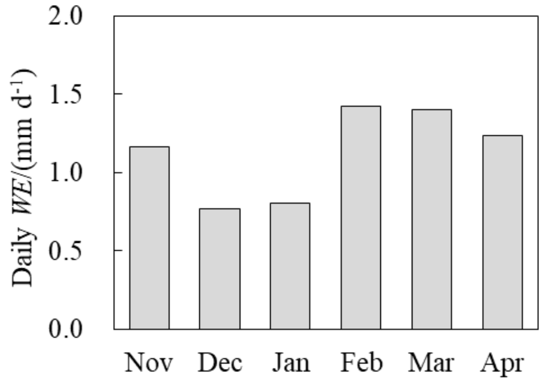

Figure 12. The daily mean surface sublimated water equivalent (*WE*) through the winter 2010–2011.